# Investigation of Metatorbernite Phase Relations in Uranium-contaminated Vadose-zone Soils

Margaux A. Bereston

The Johns Hopkins University

January 3, 2012

## Author Note

Margaux A. Bereston, Zanvyl Krieger School of Arts and Sciences, The Johns Hopkins University.

Correspondence concerning this Independent Graduate Research Project should be addressed to Margaux A. Bereston, Zanvyl Krieger School of Arts and Sciences, The Johns Hopkins University, Homewood Campus, Baltimore, MD. E-mail: mberest@jhu.edu

This research investigation was supported by U.S. Department of Energy, Basic Energy Sciences Grant DE-FG02-89ER14074 to D.R.V. and D.C.E., and the Center for Environmental Kinetics Analysis (CEKA), an NSF- and DOE-sponsored Environmental Molecular Science Institute (NSF Grant CHE04-31328 to P.J.H.). Use of the Advanced Photon Source was supported by the U.S. Department of Energy, Office of Science, Office of Basic Energy Sciences, under Contract De-AC02-06CH11357.

I would like to thank David C. Elbert, research scientist with the Department of Earth and Planetary Sciences at The Johns Hopkins University and distinguished scholar in the field of crystallography, for his commitment as Field Mentor and for providing advanced education in crystallography and X-ray diffraction techniques. Thanks also go to Joanne Stubbs from the Center for Advanced Radiation Sources (CARS) at the University of Chicago for providing expertise in preparing and staging the metatorbernite samples for X-ray diffraction at the Advanced Photon Source. This investigation is indebted to Tyrel M. McQueen from the Department of Physics and Astronomy at The Johns Hopkins University for access to the Bruker D8 Focus X-ray Diffractometer. In addition, thanks and gratitude go to Dana C. Brenner, who provided expertise in support of the fast-paced laboratory work that was required for this investigation.

**Abstract**

Uranyl phosphates of the autunite/meta-autunite group are important sinks for uranium in contaminated soils. Basic understanding of uranium migration and planning for remediation depend on recognition and understanding of these materials. The Cu meta-autunite mineral, metatorbernite [$Cu(UO_2)_2(PO4)_2 \bullet 8H2O$] comprises nearly half the solid-phase uranium budget in the contaminated vadose zone in the 300 Area of the Hanford site in Washington State, USA. *In situ*, X-ray diffraction investigation shows that temperature and activity of water ($a_{H_2O}$) are controlling parameters in the occurrence of metatorbernite. Data were collected in reflection mode with a Bruker D-8 Focus laboratory X-ray Diffractometer at the Johns Hopkins University and in transmission mode at beam line 13 BMC of the Advanced Photon Source synchrotron, Argonne National Laboratory. Temperature and $a_{H_2O}$ control and monitoring were utilized in the synchrotron experiments. Room temperature studies (~24°C) revealed intensity peaks with d-spacings 8.66 Å, 6.4 Å, and 5.4 Å. During dehydration experiments, metatorbernite heated to greater than or equal to 64°C dehydrated to a phase with d-spacings 8.3 Å, 6.9 Å, and 5.3Å. When heated above 84°C, the 6.9 Å peak increased in intensity, while the lesser hydrates of metatorbernite and its associated 8.3 Å and 5.3 Å intensity peaks lost intensity. Dehydration experiments were followed by rehydration-cooling experiments. The results indicate that lesser hydrates of metatorbernite undergo a phase change to rehydrate, as evidenced by the reappearance of intensity peaks 8.66 Å, 6.4 Å, and 5.4 Å. This phase change occurred when the temperature was lowered and the relative humidity was progressively increased.

*Keywords:* lesser hydrates, metatorbernite, uranium, vadose-zone, X-ray diffraction

# Investigation of Metatorbernite Phase Relations in Uranium-contaminated Vadose-zone Soils

Complex and problematic environmental challenges exist today due to uranium contamination in soils. Geochemical and mineralogical analyses of vadose-zone soils have determined that the majority of uranium hosts are finely grained, sparsely distributed, and intergrown with other phases (Stubbs et al., 2009). Earlier research investigations have demonstrated that natural and anthropogenically contaminated vadose-zone soils contain uranyl phosphate minerals of the autunite group that are significant hosts for uranium (Buck, Dietz, & Bates, 1995, 1996; Sato, et al., 1997; Murakami et al., 1997, 2005; Jerden et al., 2003; Jerden & Sinha, 2003; Stubbs et al., 2006, 2009; Catalano et al., 2006; Arai et al., 2007; Zachara et al., 2007; Singer et al., 2009). One of the important complexities of autunite group minerals is documented phase transitions involving variable-hydration of interlayer cations (Locock & Burns, 2003; Ross et al., 1964). While first recognized over one hundred years ago (Rinne, 1901) these dehydrations and associated structural changes remain poorly understood. These phase transitions are important, however, to understanding mineral formation and dissolution, and associated uranium sequestration or migration in contaminated soils. This study is the first investigation of the role of relative humidity on the temperatures of dehydration phase transformations in metatorbernite, the Cu bearing member of the meta-autunite group.

Autunite group minerals hold significant geochemical interest when considering the long-term transport of uranium in the subsurface environment. The stability of autunite group minerals, such as metatorbernite, can account for almost half of the uranium budget in uranium-contaminated vadose-zone soils (Catalano et al., 2006).

**Metatorbernite**

Metatorbernite [$Cu(UO_2)_2(PO4)_2 \bullet 8H2O$] forms as a result of the alteration process of torbernite undergoing dehydration. The "meta" prefix connotes the dehydrated version of torbernite as a first dehydration step. Metatorbernite is a distinct mineral host that contains uranium, phosphorous, and copper.

The structure of metatorbernite consists of sheets that contain uranyl square bipyramids linked by phosphate tetrahedra (Ross et al., 1964; Stergiou, Rentzeperis, & Sklavounos, et al., 1993; Locock & Burns, 2003). The uranyl square bipyramids share their corners with the phosphate tetrahedral corners. The uranyl phosphate sheets of metatorbernite are held along the (001) basal cleavage plane by van der Waals bonds forming mica-like layers with the interlayer area occupied by $Cu^{2+}$. The Cu is also bound by the two apical uranyl oxygen from the uranyl phosphate sheets (Locock and Burns, 2003). The $Cu^{2+}$-O bond is strong because of its covalent nature.

The interlayer contains independent molecular water groups held in place by no more than hydrogen bonding (Locock & Burns, 2003; Suzuki et al., 1998, 2005). There are two types of water molecules in metatorbernite. The first type involves four water molecules coordinated around $Cu^{2+}$ in the interlayer. The second type of water molecule is not coordinated with $Cu^{2+}$ and is presumably held on the interlayer only by hydrogen bonding (Locock & Burns, 2003).

Metatorbernite is found both in naturally and anthropogenically contaminated environments, as well as via synthetic laboratory production that utilizes slow diffusion of $H_3PO_{4(aq)}$ into copper-bearing silica gel (Locock & Burns, 2003).

**Natural Occurrence.**

Metatorbernite ore is found in fracture zones undergoing hypogene-supergene mineralization. It can form as a result of the following conditions: (a) changes in the solubility of a solution of uranium, which can occur via groundwater and deposition, (b) evaporation of ground water that bears uranium, or (c) *in situ* oxidation of hydrothermal solutions containing tetravalent uranium (Walker & Osterwald, 1956). Metatorbernite is classified as a secondary uranium mineral that is found in both pegmatite veinlets and hydrothermal pitchblende veins.

The abundance of copper in the environment promotes the formation of the copper-autunite mineral metatorbernite $Cu(UO_2)_2(PO4)_2 \cdot 8H2O$. The ability of metatorbernite to nucleate and form in an ore depends upon the presence of copper as a constituent of the chemical composition of the geological system, as well as the activity of water. Over time, the combinations of weathering and hypogene-supergene processes expose veins and veinlets, which lead to natural dispersal.

*Figure 1.* Metatorbernite here, (Copyright 2009 mindat.org).

Many of the finest metatorbernite samples in the world come from the Democratic Republic of the Congo. Its natural ore is radioactive and owes its dark green color to oxidation of $Cu^{2+}$ (see Figure 1).

**Anthropogenic Contamination.**

Nuclear weapons production is one of the most significant anthropogenic sources of radioactive contamination in the United States (DOE 1997). The U.S. DOE estimates that approximately 63$Mm^3$ of soil and 1,310 $Mm^3$ of groundwater are contaminated (U.S. Department of Energy, 1997 a, b). The DOE manages the material within a complex of 64 contaminated sites in 25 states (U.S. Department of Energy, 1997 a, b).

Anthropogenic contamination has occurred, among other locations, at the U.S. Department of Energy (DOE) Hanford Site, a nuclear weapons production facility in the State of Washington. At the Hanford Site, production of nuclear weapons has created one of the largest contamination sites in the U.S., resulting in expensive remediation programs costing over $100 billion (Crowley, 2007).

Leading up to and during World War II, the DOE Hanford Reservation site in Washington State housed plutonium production reactors adjacent to the Columbia River in 100 Area; buried high-level waste (HLW) from nuclear spent fuel in underground tanks in 200 Area;[1] and fabricated nuclear fuel in 300 Area. The anthropogenic radioactive contamination in 300 Area occurred through waste stream discharge of acidic uranyl-copper, during the dissolution of

[1] High level waste (HLW) is highly radioactive material that is the byproduct of reactions occurring inside the nuclear reactors, such as spent nuclear fuel ready for disposal and waste materials that remain from spent fuel reprocessing for the production mixed oxide fuels (NRC, 2011).

nuclear fuel and fuel rod cladding (Wellman et al., 2009; Zachara et al., 2005). The subsurface environment requires remediation in both vadose-zone soils and groundwater.

**Research Purpose**

The overreaching goal of this investigation is to improve engineering remediation models that utilize phosphate amendments that reduce toxic metal mobility of uranium-bearing contamination in the environment. This research investigation will contribute to ongoing research for improved bulk kinetic models for remediation of both natural and anthropogenic contamination of vadose-zone soils. For example, at the Hanford Site 300 Area, the data will assist with remediation technologies that are designed to prevent or slow uranium-containing hydrogeologic plume migration into groundwater and into the Columbia River.

**Research Plan**

The first goal of this investigation is to determine the temperatures of dehydration transitions of the lesser hydrates of metatorbernite as a function of the activity of water ($a_{H_2O}$). The second goal is to investigate whether observed states of dehydration are reversible through the process of rehydration and to what degree of rehydration, if it occurs, results in a phase that is equivalent to the original metatorbernite sample.

The research specimen for this investigation is natural metatorbernite ore from the Musonoi Mine, Katanga Province, Democratic Republic of the Congo. The unit cell structure of the sample was determined by X-ray Powder Diffraction (XRD) utilizing Le Bail fit and TOPAS software to be P4 with a cell volume of 839.63121 Å, a = 6.095 Å, b = 6.095 Å, and c=17.307.

Previous studies have determined neither the reversibility of lesser hydrates of metatorbernite, nor the role of water activity in metatorbernite phase relations. Recent work

(Stubbs et al., 2010) demonstrated that the second dehydration of metatorbernite involves reconstruction of autunite-type sheets to uranophane-type sheets. For comparison purposes with previous studies conducted by Stubbs, et al. (2010), diffraction patterns in the investigation included basal spacings of 8.7 Å, 8.3 Å, and 6.9 Å coupled with a temperature range of 23.5°C and 110°C.

## Experimental Methods

This investigation included metatorbernite sample preparation, heating studies, and relative humidity control. X-ray diffraction (XRD) and synchrotron X-ray diffraction were utilized to determine the impact that increasing temperature had on basal spacings, as well as the degree of the collapse demonstrated by shifting diffraction patterns.

### Bruker X-ray Powder Diffraction.

Powder diffraction data was collected at The Johns Hopkins University, Department of Physics and Astronomy using a Bruker D8 Focus X-ray Diffractometer analyzer. Quantitative analysis was performed with DIFFRAC$^{plus}$ Software utilizing DIFFRAC$^{plus}$ EVA and TOPAS programs.

Analysis of powder diffraction utilized Bragg's Law, $2d\sin\theta = n\lambda$. Measurements provided the intensity distribution related to the angle $2\theta$. The Bruker XRD was calibrated with a NIST standard reference piece of $Al_2O_3$, and the X-ray wavelength for the experiments was 1.5406 Å. The maximum absolute error in $2\theta$ positions corresponds to 0.01% d-spacing error (Dr. Tyrel McQueen, personal communication, 2011). Calibration of the diffractometer was done with the NIST 1987a alumina standard and no internal standards were used.

***Preferred Orientation.***

X-ray diffraction of powdered metatorbernite is hampered by preferred orientation. When crystals of metatorbernite lie flat on their cleavage surfaces preferred orientation occurs. Preparation of metatorbernite powder required not packing the samples onto the sample holder, due to their tendency to undergo preferred orientation. To minimize preferred orientation, the powder sample is rotated inside the Bruker XRD analyzer, while diffraction patterns are collected.

***Offsets.***

While precise location of intensity peaks is desirable, our patterns are subject to small offsets in $2\theta$ position. These offsets can arise due to either variation in sample height, the presence of macroscopic strain, or poor calibration of the $2\theta$ scale.

In this investigation, sample height was somewhat poorly controlled, because samples were not packed to minimize preferred orientation. In addition, in this study metatorbernite samples were ground dry to avoid potential adulteration of sample hydration state. The use of a grinding fluid typically minimizes induced strain in samples and so dry grinding may have contributed to $2\theta$ offsets. While there are several reasons for offsets to occur, the majority of the strain in our metatorbernite may have been induced by the dry grind process (see Figure 2).

The ground metatorbernite power was loaded on to a 22 mm round glass slide, inserted into the chuck, and heated to established temperatures in preparation for XRD scanning. Samples were scanned from 5° to 60° $2\theta$ for four minutes. The "step size" was 0.016˚ and the "time of step" was 0.07 sec. X-ray wavelength was 1.5406.

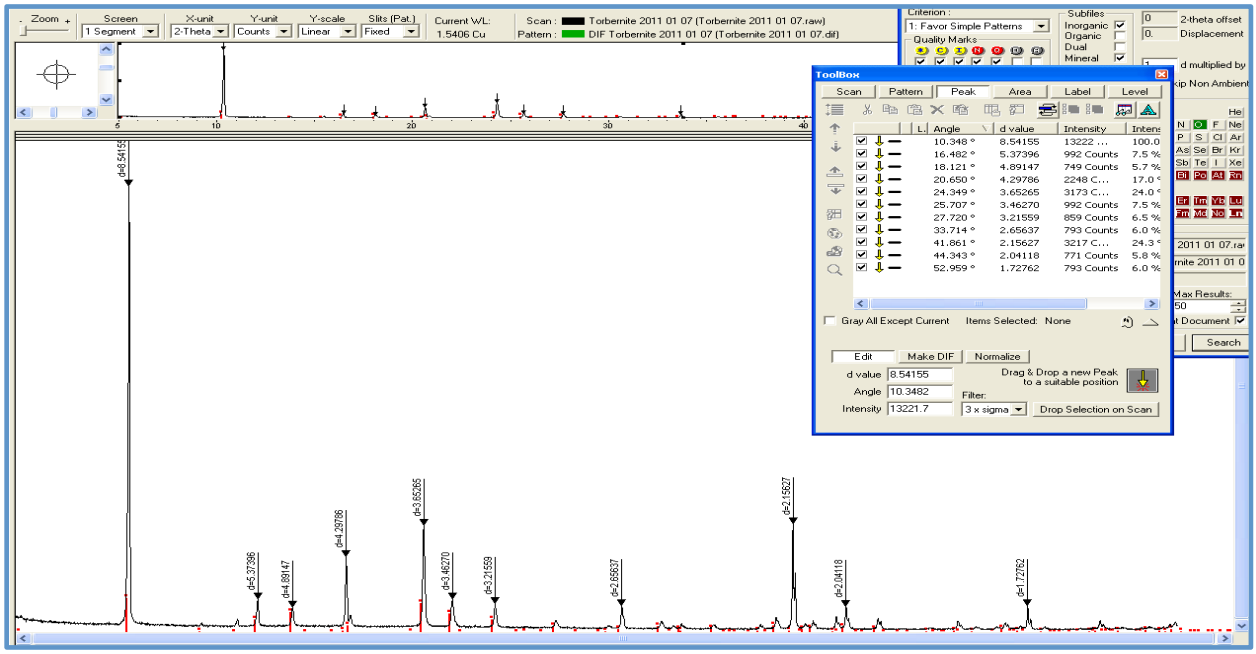


*Figure 2* Metatorbernite Bruker XRD Offsets Shown in Red.

***Sample Preparation.***

Flakes of metatorbernite removed from the ore sample were ground "dry" with an agate mortar and pestle for preparation of samples containing pure metatorbernite crystals. In order to prevent unwanted microscopic constituents of the ore from contaminating the pure meta-torbernite samples, a Zeiss Model 47 50 52 microscope provided visual inspection of the uniformity and purity of the grind. Upon completion of this process, both flakes and ground crystals of metatorbernite were stored in sealed glass vials.

**Heating Studies.**

The purpose of the heating studies was to induce dehydration in powdered metatorbernite samples and quantitatively analyze the temperatures of transition. Transitions were marked by changes in basal spacing. This type of change in the basal spacing may be seen in the diffraction pattern as metatorbernite dehydrates into its lesser hydrates. Peak broadening, though the overall

intensity remains constant, may occur as a function of stepping up into increasing temperature settings that cause dehydration of the unit cell along the c-direction.

Initial heating temperature settings of 23.5°C, 110°C, and 140°C were selected to match the transitions noted by Stubbs et al. (2010). During the 140°C heating experiment, it was determined, that the chuck used in the Bruker D8 X-ray Diffractometer could not be scanned at set point temperatures above 140°C.[2] Revised temperatures of 48°C, 85°C, and 110°C were established for all further XRD heating studies, due to the thermal limitations of the chuck. The metatorbernite powder was heated on hotplates that were calibrated for temperature using PTC Instruments Spot Check, Model 572C and a Fluke 51 II thermometer. A significant shortcoming of the experiments was the lack of an *in situ* heating device. Heating was done outside the diffractometer. Samples were transferred to the instrument as quickly as possible, but it was impossible to effect precise control over the experimental temperatures this way.

***Heating Study 1 – Step Up 48°C, 85°C, and 110°C Dehydration.***

Metatorbernite powder was heated on a small Thermo Scientific hot plate to 48°C for 10 minutes, scanned, and the diffraction pattern read. The procedure of heating and XRD scanning was repeated for the same sample after stepping up into higher temperature settings of 85°C and 110°C. The resulting three diffraction patterns are shown in overlay for d-spacings 8.5 Å (48°C), 8.2 Å (85°C), and 6.82 Å (110°C) intensity peaks in Figure 3. The differences in the three diffraction patterns indicated that distinct changes took place within the unit cell structure during the heating experiments (see Figure 3). Diffraction peak 8.5 Å (48°C) corresponds to

[2] The chucks are round steel disks with aluminum centers. A 22 mm round glass slide fits into the aluminum center of the chuck, see Figure 3. The two metals and the glass slide have different thermal properties that limited the maximum temperature of the chuck to 140°C in the Bruker XRD.

metatorbernite, and diffraction peaks with d-spacings 8.2 Å (85°C) and 6.82 Å (110°C) correspond to lesser hydrates of metatorbernite.

In analyzing the results, the d-spacing 6.82 Å (110°C) peak had an intensity remnant of 815 reflections from the 8.2 Å (85°C) peak, while measurable intensity was not demonstrated in the diffraction pattern from the original 8.5 Å (48°C) d-spacing peak. The complete loss of the 8.5 Å d-spacing intensity peak indicated that metatorbernite when heated to 110°C consisted only of the metatorbernite's lesser hydrates.

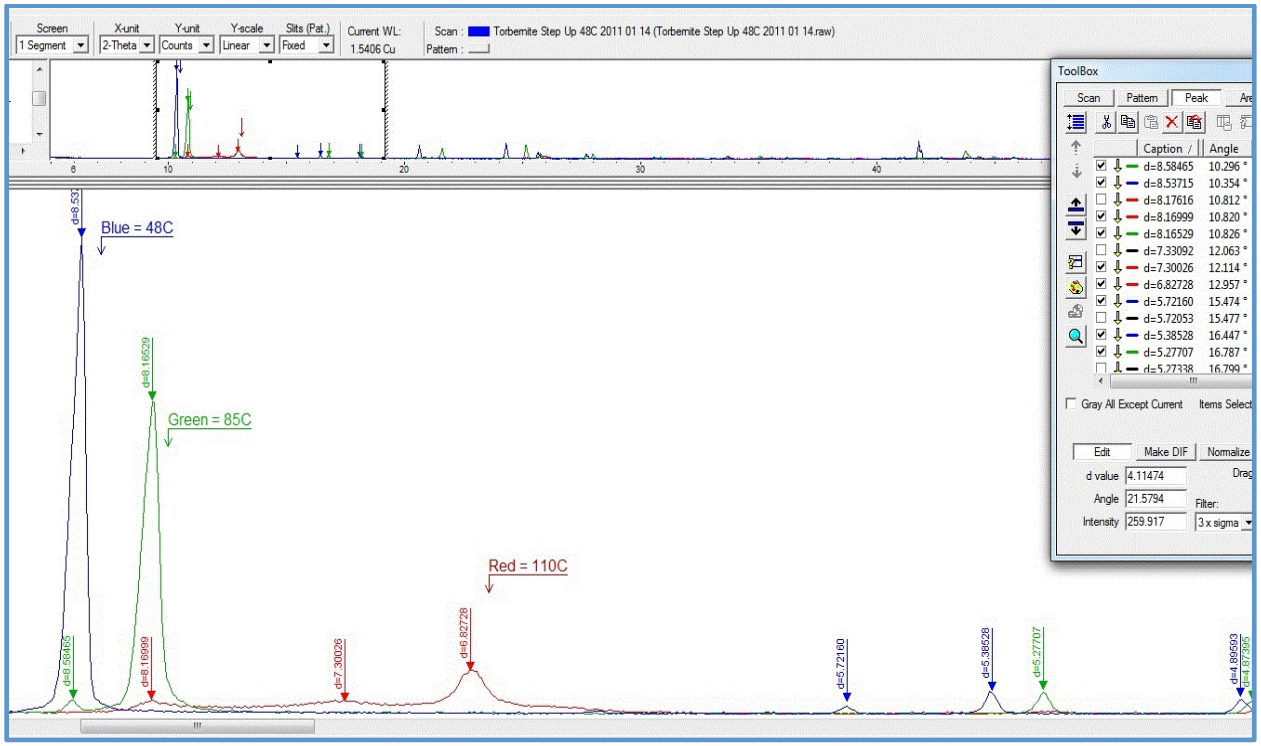


*Figure 3.* Step Up Heating Experiment 1, Overlay of 48°C, 85°C, and 110°C.

The d-spacing for the 8.2 Å (85°C) peak had an intensity remnant of 856 reflections from the original 8.5 Å (48°C) peak. The retention of small amounts of peak intensity indicated that incomplete reactions occurred between 48°C, 85°C, and 110°C. Furthermore, the results indicated that utilizing smaller temperature increments in subsequent experiments would quantitatively capture the transitions of the lesser hydrates of metatorbernite.

A significant finding was that both the 8.3 Å d-spacing and the 6.9 Å d-spacing intensity peaks appear at lower temperatures than had been demonstrated in previous investigations by Stubbs et al. (2010), Suzuki et al. (2005), and Locock and Burns (2003). An additional finding in this heating study was that it confirmed the existence of peak intensities with d-spacings smaller than 6.9 Å, (i.e., 5.4Å), which was in agreement with Suzuki et al. (2005).

***Heating Study 2 - 150°C Dehydration with RH Controlled Environment.***

Ground metatorbernite set on a slide inside a small, aluminum foil oven was heated for 96 hours at 150°C on a foil wrapped VWR Scientific Products, Model 370 Hotplate/Stirrer. After 96 hours, the metatorbernite was loaded on to a chuck, scanned, and the diffraction pattern (red) was read (see Figure 4).

The red diffraction pattern, with a temperature of (~140°C during XRD scan) 150°C (0 minutes), demonstrated that the 8.7 Å d-spacing had undergone almost a total loss of intensity, which is associated with dehydration in the basal spacing of the unit cell structure.

Without residual or remnant transitions peak intensities appearing in the red diffraction pattern, it was evident that heating metatorbernite to 150°C caused the complete disappearance of d-spacing 8.7 Å (RT) intensity peak. In analyzing the results, the appearance of the 6.9 Å (150°C) diffraction pattern (red) indicated that only the lesser hydrates of metatorbernite were present (see Figure 4).

After completion of the 150° heating experiment, the sample was sequestered and sealed in the environmental chamber with a beaker of water for 48 hours at room temperature to determine if the metatorbernite was undergoing rehydration. After 48 hours in the chamber, the subsequent diffraction pattern (black) indicated that the metatorbernite hydrate was reconstituting, as evidenced by the decreased intensity of the lesser hydrate with d-spacing 6.9 Å

(150°C). In addition, there were intensity peaks that had undergone peak broadening and increases in intensity.

After the metatorbernite sample spent an additional 96 hours in the sealed, environmental chamber with a beaker of water, it was XRD scanned and the diffraction pattern (black) was taken to determine if any further rehydration took place. In Figure 5, the original 6.9 Å (150°C) d-spacing diffraction pattern (red) is overlaid with the 96-hour diffraction pattern (black).

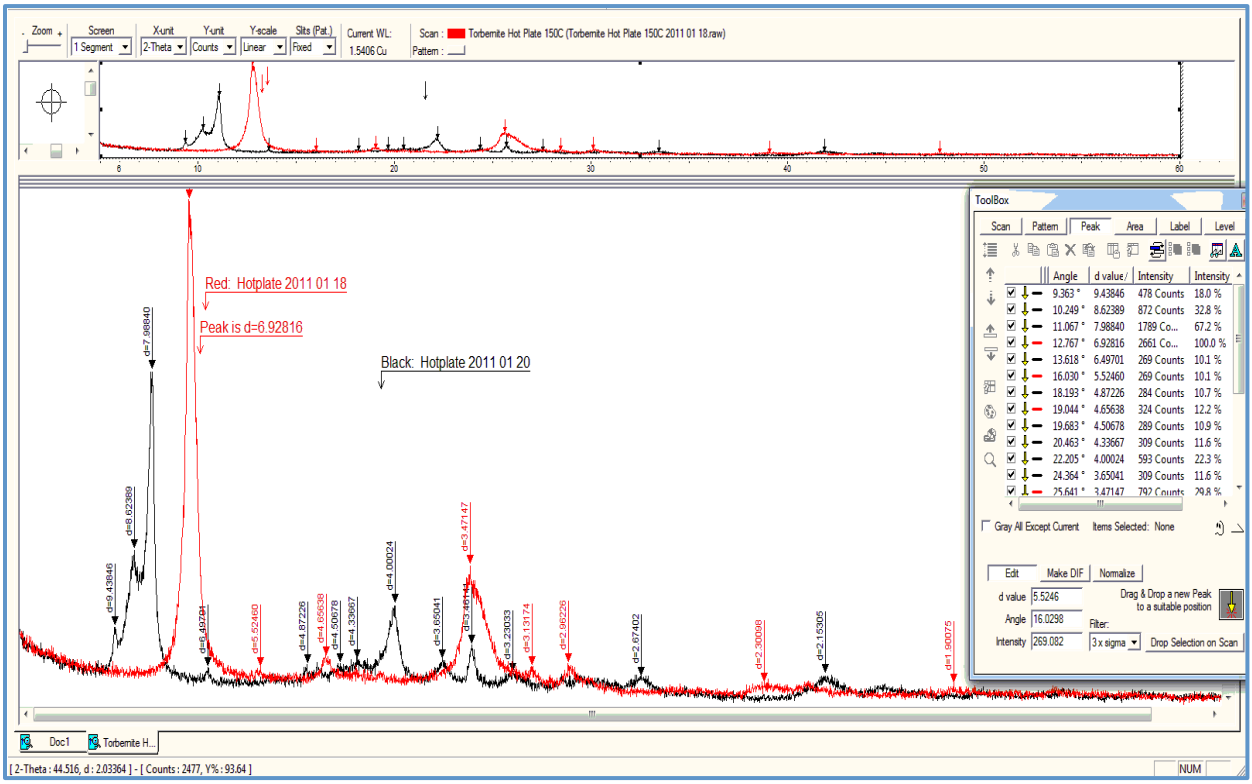


*Figure 4.* 150°C Dehydration Diffraction Pattern (red) and Rehydration Diffraction Pattern (black) after 48 Hours.

The 48-hour and 96-hour black diffraction patterns (see Figures 4 and 5) demonstrated that significant transitions occurred, while the sample rehydrated to metatorbernite hydrate at room temperature (~21°C). For example, during the 96-hour rehydration phase, the 6.9 Å (150°C) basal spacing transitioned from the lesser hydrate of metatorbernite to d-spacings 8.0 Å and 8.7Å (RT). This finding suggests that the metatorbernite is reconstituting.

When the red and black diffraction patterns were compared, the 8.0 Å d-spacing peak and the 8.7Å (RT) d-spacing peak demonstrated that some metatorbernite hydrate had reconstituted, although some metatorbernite peaks were broader and less distinct during rehydration (see Figures 4 and 5). The intensity peaks for d-spacings 8.6 Å and 6.9 Å indicated that an insignificant change in the amount of reconstituted metatorbernite hydrate had formed between 48 hours and 96 hours.

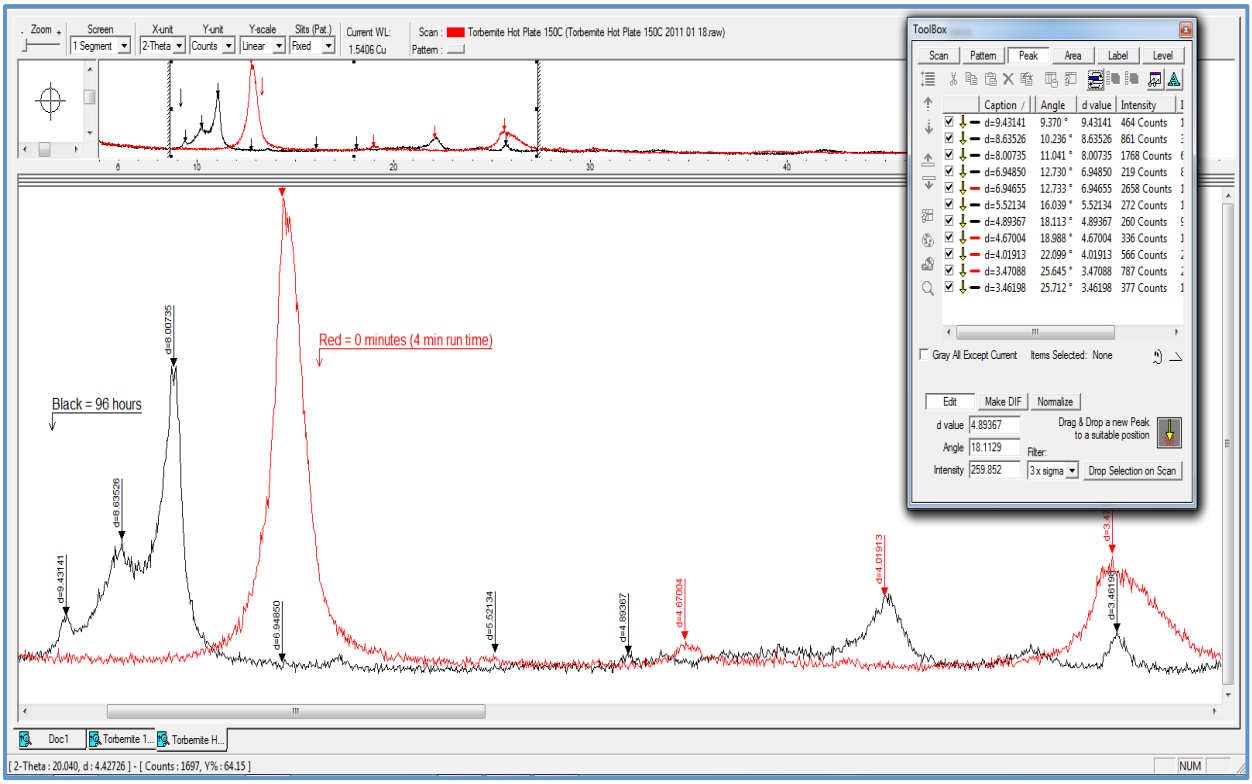


*Figure 5.* 150°C Dehydration Diffraction Pattern (red), Overlaid with Rehydration RT Diffraction Pattern (black) after 96 Hours (zoomed).

For example, comparing the intensity of d-spacing 6.9 Å at 48 hours (black diffraction pattern) with the intensity of d-spacing 6.9 Å at 96 hours (black diffraction pattern) there were 269 reflections and 219 reflections respectively; therefore, the two intensities are not markedly different. This indicated that most of the rehydration in metatorbernite is taking place within the first 48 hours.

The rehydration results of this experiment have not been previously demonstrated. The appearance of reconstituted metatorbernite hydrate via rehydration indicated that dehydration to the lesser hydrates of metatorbernite was reversible. Some of the rehydration may be attributed to the addition of $H_2O$ molecules adjacent to $Cu^{2+}$ in the basal spacings. If this were the case, dehydration followed by rehydration could be altering the unit cell diffraction pattern of metatorbernite. Furthermore, the results of this heating study are in agreement with "Heating Study 1" in that intensity peaks with basal spacings lower than 6.9 Å, (i.e., 5.4 Å and 5.3 Å) were demonstrated.

The results of the dehydration portion of the 150°C heating experiment, particularly the appearance of the 6.9 Å (150°C) basal spacing, are consistent with previous investigations by Stubbs et al. (2010), Suzuki et al. (2005), and Locock and Burns (2003). However, the appearance of lesser hydrates of metatorbernite occurred at lower temperatures than previous investigations by Stubbs et al. (2010), Suzuki et al. (2005), and Locock and Burns (2003).

***Heating Study 3 – 140° Dehydration, RT Passive Rehydration.***

Metatorbernite powder was placed on a 22 mm glass slide and loaded onto a chuck. The chuck and slide assembly were heated to 140°C on the Thermo Scientific hot plate. A SpotCheck Thermostat confirmed the sample was 122°C during the XRD scan. During this experiment, the metatorbernite cooled passively at room temperature inside the Bruker XRD environment. The sample was scanned every 15 minutes for 260 minutes (see Figure 6) followed by a final diffraction pattern taken at 1017 minutes (see Figure 7).

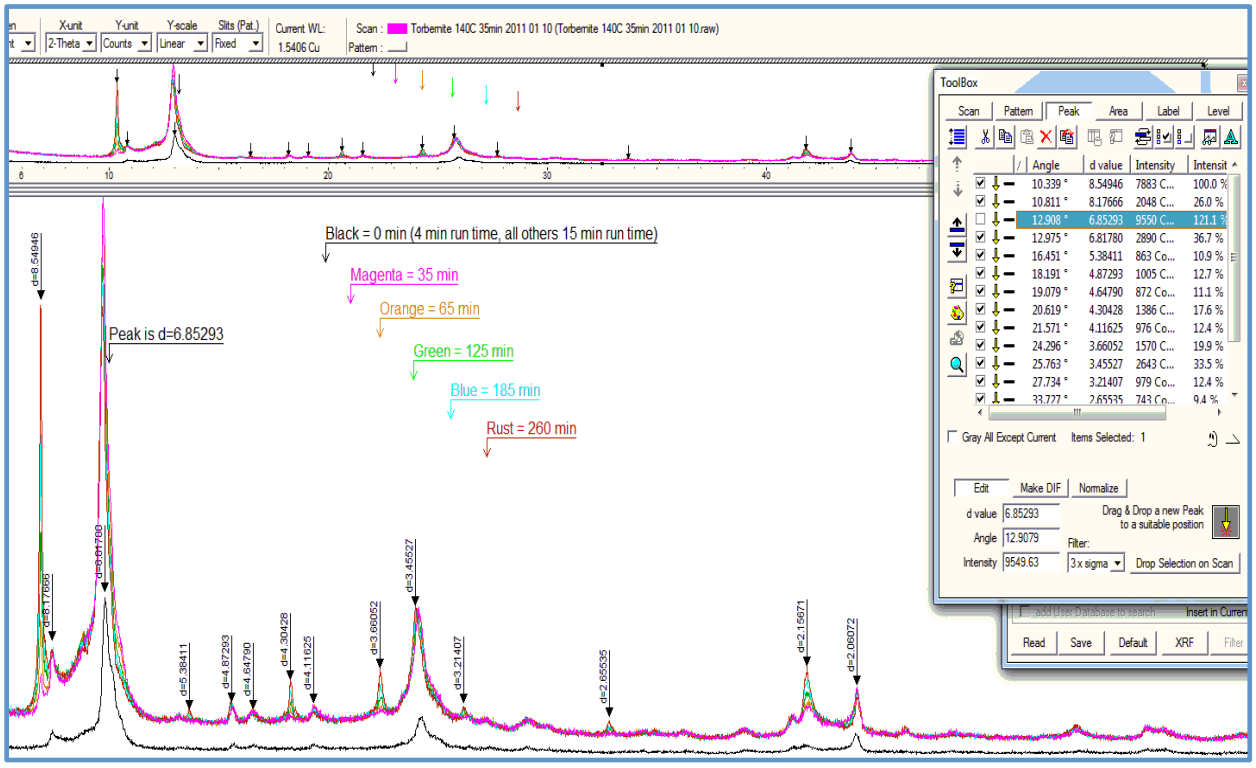


*Figure 6.* 140°C Heating Study 3 - Dehydration Diffraction (black) and Cooling Diffraction Patterns to 260 Minutes.

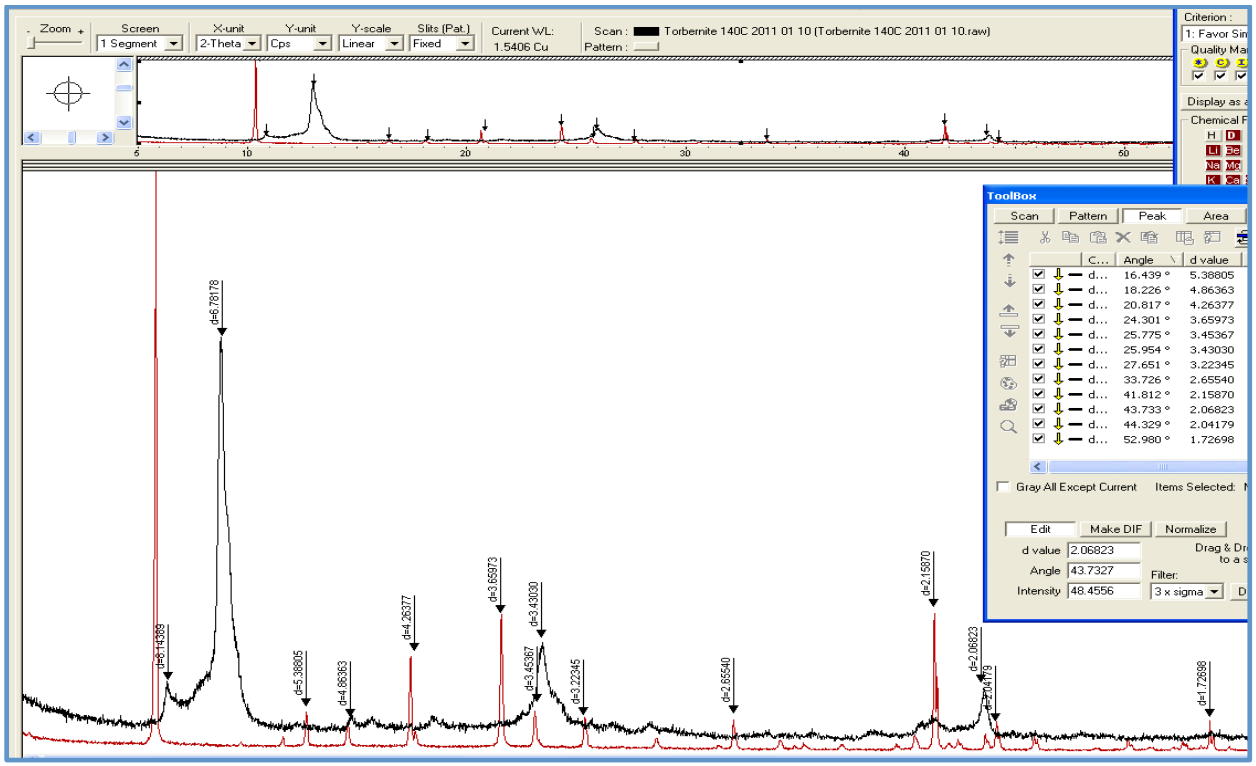


*Figure 7.* 140°C Heating Study 3 – 1017 Min. Dehydration Diffraction Pattern (black) and Final RT Diffraction Pattern.

Analysis of the diffraction patterns in this experiment indicated that incremental rehydration took place. The lesser hydrates of metatorbernite with d-spacings 8.5 Å, 8.2 Å, and 6.82 Å were losing intensity as the sample cooled and rehydrated. During rehydration and cooling of the metatorbernite at RT (23.8°C), the 8.5 Å d-spacing (see Figures 6 and 7) indicated that reconstitution of metatorbernite hydrate was taking place.

This result further supports the reversibility of metatorbernite's lesser hydrates and the reconstitution of metatorbernite hydrate, during the rehydration-cooling experiment phase after 48 hours (see Figure 8). These findings will be further tested for consistency and repeatability, during experimentation at the Advanced Photon Source (APS).

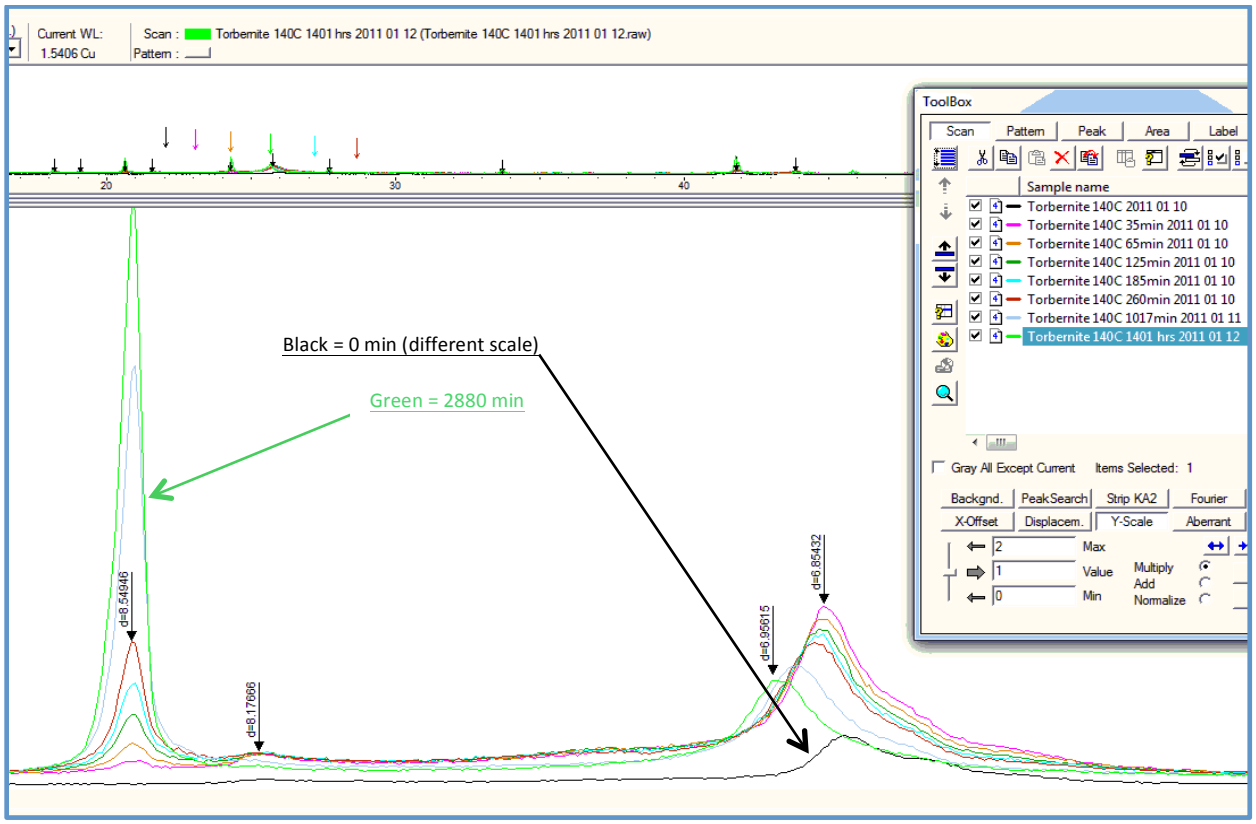


*Figure 8.* 140°C - 48 Hour Rehydration.

**Rehydration RH Study – Sealed Environmental Chambers.**

During the three heating studies, analysis of the diffraction patterns indicated that some rehydration was taking place within the basal spacings as the samples cooled. Metatorbernite heated to specific temperatures, cooled passively to room temperature while inside the Bruker XRD during subsequent scans. The diffraction patterns demonstrated evidence of rehydration that was passive, slow, and subject to dry conditions in the solid-state chemistry lab caused by numerous baking furnaces.

In light of these observations, a method for controlling and analyzing the activity of water in metatorbernite for two specific set points of relative humidity was required. Two sealed environmental chambers were setup to control the activity of water ($a_{H_2O}$) at room temperature. Supersaturated solutions of lithium chloride and potassium chloride, providing relative humidity of 11.3% and 84.3% respectively, were chosen to maintain the relative humidity in the sealed environmental chambers (Greenspan, 1977). Beakers of the two solutions were prepared and placed in the sealed chambers for 24 hours of acclimatization, prior to the introduction of metatorbernite samples. Once in the chambers, a Traceable Humidity-On-A-Card monitored the relative humidity. The two samples were freshly ground and each placed in a dedicated, sealed environmental chamber. The samples remained in the chambers for five days to acclimate.

***RH Experiment 1– Two Sealed Environmental Chambers.***

In "Chamber 1", LiCl maintained relative humidity at 11.3%. After acclimating for 120 hours, the metatorbernite sample looked drier. One-half of each sample was XRD scanned, and the diffraction pattern taken. In the LiCl 11.3% RH environment, the diffraction pattern for d-spacings 8.56 Å and 6.38 Å had peak intensity reflections of 3514 and 322 respectively (see Table 1 and Figure 9).

"Chamber 2" contained KCl that maintained relative humidity at 84.3%. After 120 hours, the metatorbernite sample looked the same as the sample from Chamber 1. One-half of each sample was XRD scanned, and the diffraction pattern taken. In the KCl 84.3% RH environment, the diffraction pattern for d-spacings 8.56 Å and 6.38 Å had a peak intensities of 1999 and 270 respectively (see Table 1 and Figure 9).

Table 1.

*Chamber 1 and Chamber 2 Peak Intensity Comparison.*

| **Chamber** | **Environment RH** | **8.6 Å Intensity** | **6.4 Å Intensity** | **5.4 Å Intensity** |
|---|---|---|---|---|
| 1 | LiCl 11.3% | 3514 | 322 | 1361 |
| 2 | KCl 84.3% | 1999 | 270 | 1163 |

In Chamber 1 the peak intensities (black) for d-spacings 8.6 Å, 6.4 Å, and 5.4 Å are higher at room temperature when low relative humidity is 11.3%. In Chamber 2, the peak intensities (red) for d-spacings 8.6 Å, 6.4 Å, and 5.4 Å are lower at room temperature when the relative humidity is 84.3%, although the difference was mostly evident in the d-spacing 8.6 Å intensity peak (see Table 1 and Figure 9).

The diffraction patterns from both chamber experiments demonstrated d-spacings 8.6 Å, 6.4 Å, and 5.4 Å peak intensities that were indicative of metatorbernite hydrate at room temperature (see Figure 9). Further confirmation of metatorbernite is demonstrated by the absence of its lesser hydrates with d-spacings 8.2 Å, 6.9 Å, and 5.3 Å in the diffraction patterns (see Figure 9).

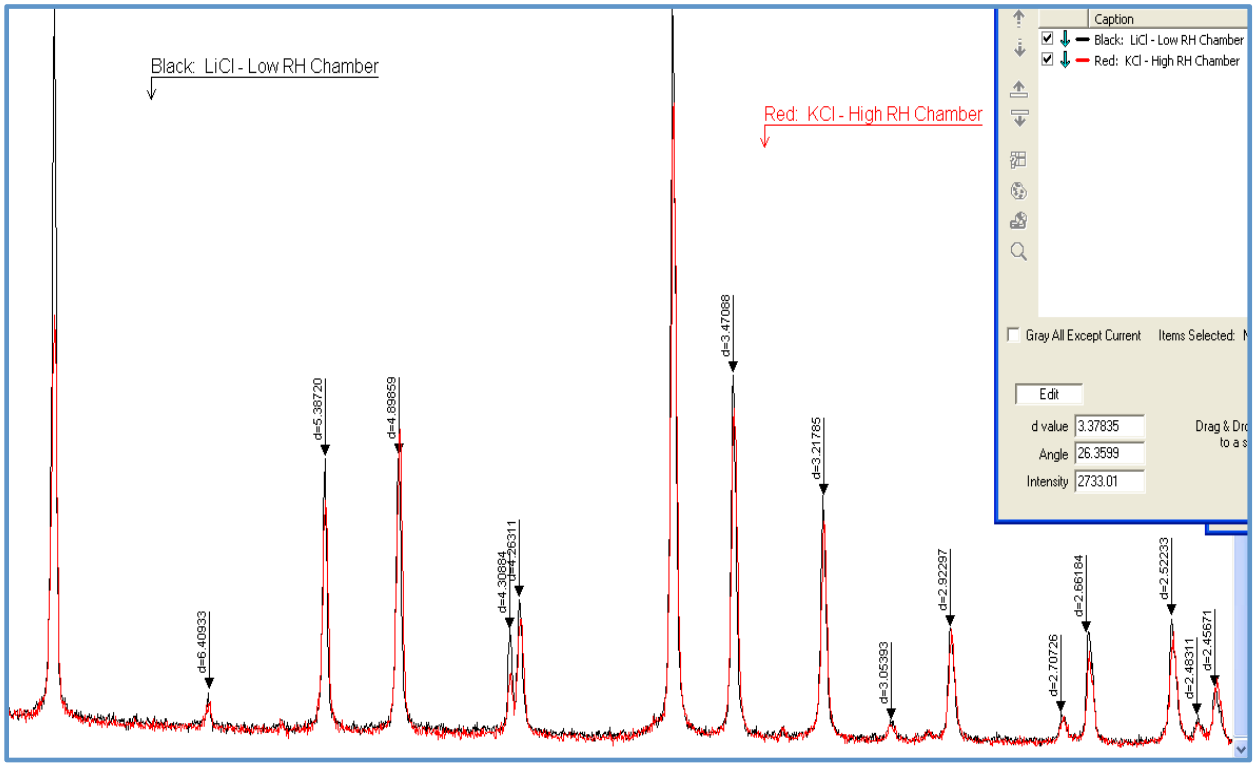


*Figure 9.* Overlay of LiCl (black) and KCl (red) RH Diffraction Patterns.

The results from this experiment indicated that lesser hydrates of metatorbernite were not present when the relative humidity was ≥11.3% and ≤84.3% at room temperature. These results were different from the 150°C, 140°C, and Step-up heating experiments when higher temperatures induced transition conditions that resulted in the appearance of lesser hydrates of metatorbernite. In this experiment, the peak intensities (red) for d-spacings 8.6 Å, 6.4 Å, and 5.4 Å in Chamber 2 with high relative humidity are lower at room temperature, though the difference was mostly evident in the d-spacing 8.6 Å peak intensity.

***RH Experiment 2 – Switched Environmental Chambers.***

Upon completion of the XRD scans, the remaining halves of both the original metatorbernite powder samples from the LiCl (low 11.3% rh) in Chamber 1 and the original metatorbernite powder from the KCl (high 84.3% rh) in Chamber 2 were weighed, placed on

new slides, and switched to the opposite chambers. After acclimating for 96 hours in each sealed chamber, the metatorbernite samples were XRD scanned and the diffraction patterns read.

When the sample originally from Chamber 2 high RH KCl (lower peak intensity-red pattern) was placed in Chamber 1-low RH LiCl, the intensity of the 8.5 Å d-spacing peak (green pattern) increased (see Table 2 and Figure 10). The increase in peak intensity demonstrated that the metatorbernite lost water in the low humidity environment of Chamber 1. This result was consistent with RH Experiment 1.

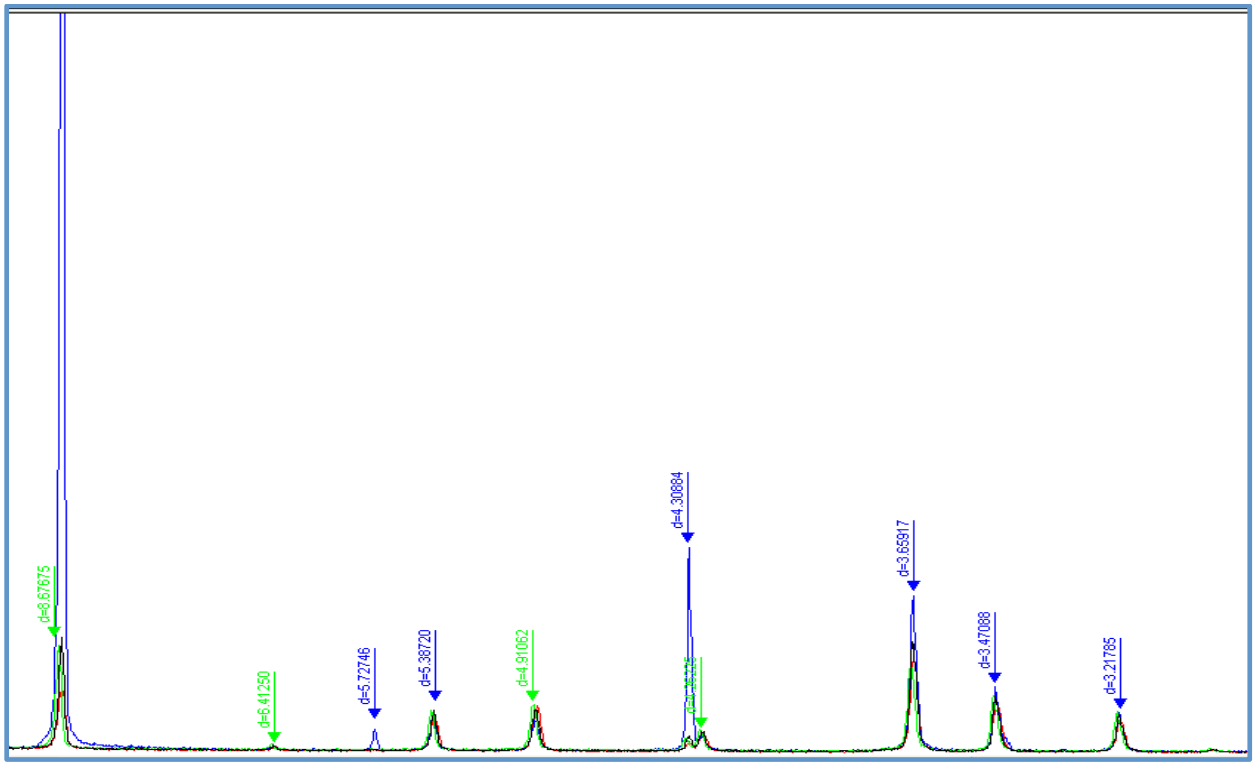


*Figure10.* Chamber 1 and Chamber 2 - D-spacing.

However, when the Chamber 1 low RH LiCl sample (original higher peak intensity-black pattern) was placed into Chamber 2 high RH KCl, the 8.5 Å d-spacing peak (blue diffraction pattern) broadened and increased in intensity by a small amount (see Figure 10). This result was

not consistent with RH Experiment 1. It is possible that at room temperature the sample would not undergo rehydration when it was switched into Chamber 2 (high RH). The four diffraction patterns from the Chamber 1 and Chamber 2 experiments were overlaid in Figure 10. Le Bail fit was utilized to compute the dimensions for each unit cell (Table 2). There were only the slightest measureable differences between the dimensions of the unit cells (see Figure 11).

Table 2.

*Metatorbernite Unit Cell Dimensions per Chamber 1 and 2.*

| **RH Experiment 1** | **Chamber Number** | **Environment RH** | **Unit Cell a, b** | **Unit Cell a, b** |
|---|---|---|---|---|
| | 1 (29) | LiCl 11.3% | 6.9623 | 17.3043 |
| | 2 (25) | KCl 84.3% | 6.9635 | 17.3090 |
| **RH Experiment 2** | **Chamber Number** | **Environment RH** | **Unit Cell a, b** | **Unit Cell a, b** |
| | 1(29) | LiCl 11.3% | 6.9652 | 17.3068 |
| | 2(25) | KCl 84.3% | 6.9652 | 17.3072 |
| | | | | |

The results of the sealed environmental chamber studies are significant because the investigations controlled temperature and two fixed points of relative humidity, the latter being less of a factor at room temperature (~24°C) with chamber fixed-point values of RH 11.3% and RH 84.3%. When comparing diffraction patterns of Chamber 1 (11.3% RH) with Chamber 2 (84.3%), the results had a high degree of correlation with respect to the dimension of the unit cell structure (see Table 2 and Figure 11).

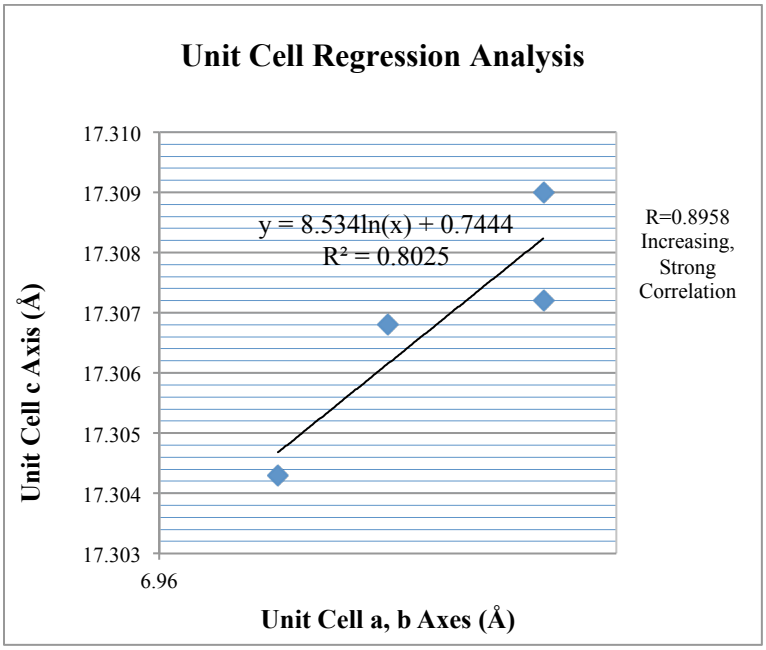


***Figure 11.*** Metatorbernite Unit Cell Regression Analysis.

**Advanced Photon Source Experiments.**

Synchrotron experiments were performed at the Advanced Photon Source, Argonne National Laboratory. The APS investigation provided better control of both relative humidity and temperature, in order to gain better insight into the effect of relative humidity on transition temperatures. Incremental dual control of $a_{H_2O}$ and temperature on the phase changes of metatorbernite has not been addressed in previous investigations.

The images were recorded with a Mar charge-coupled device (MarCCD) that was masked with an aluminum foil filter. The temperature range of the APS experiments was from 26°C to 100°C with fixed-point temperatures of 26°C, 36°C, 64°C, 68°C, 72°C, 76°C, 80°C, 84°C, and 100°C, while controlling the activity of water ($a_{H_2O}$) by flowing dry gasses through the sealed environmental cell. The maximum temperature of the gas flowing through the cell was 100°C.

A containment cell environment that was used for previous experiments with radioactive samples was modified for the metatorbernite diffraction experiments. The cell consisted of an aluminum body, a Kapton dome, and a filtered inlet/outlet system for the introduction of wet and dry gasses. The Kapton dome permitted transmission of incident and diffracted X-rays during experimentation. The maximum operating temperature of the Kapton tape dome was 400°C. The instrumentation for the cell included a strip heater, thermocouple, and relative humidity sensor (Honeywell HIH-4000-003). Thermocouples were calibrated to the cold junction of the Keithley Model 2701 used for monitoring. Factory calibration was used for the relative humidity sensor. The Honeywell relative humidity sensor was calibrated with an unscaled index that resulted in negative RH values in the data. The unscaled relative humidity data in the APS portion of this investigation is designated as "RHi".

Low relative humidity delivered via dry helium gas with a flow rate of 0.075 SCFH (Standard Cubic Feet per Hour) provided fine-tuning of the relative humidity, particularly during dehydration followed by rehydration-cooling cycle experiments. Raising the relative humidity ($a_{H_2O)}$ of the environmental cell utilized wet helium gas with a flow rate of 0.075 SCFH. Low- and high-humidity experiments at APS included tighter control of relative humidity and temperature, leading to better, more detailed analysis of metatorbernite and its lesser hydrates. In comparison, similar experimental data collected from the Bruker X-ray Diffractometer produced data for RT (~24°C), fixed-point temperatures of 48°C, 85°C, and 110°C, and two relative humidity ($a_{H_2O)}$ set points of 11.3% and 84.3% only.

The X-ray wavelength was 0.8321 Å. Diffraction lengths were calibrated with $CeO_2$. CCD data were reduced to one-dimensional scans using FIT2D (Hammersley, A.P., Svensson,

S.O., Hanfland, M., Fitch, A.N., & Hausermann, 1996). Exposure times varied from 5 to 120 seconds.

***Sample Preparation.***

The sample preparation required removal of metatorbernite from the ore sample. Samples were ground "dry" with an agate mortar and pestle and the Zeiss Model 47 50 52 microscope confirmed the uniformity and purity of the grind. The metatorbernite samples were shipped to the University of Chicago for loading into a sealed containment environment cell for analysis at the Advanced Photon Source. A thin layer of metatorbernite powder was affixed to Kapton tape set in an O-ring. Affixing the sample to the tape provided superior control over the thickness in comparison to the Bruker D8 sample chucks. The metatorbernite powder sample was placed in the environmental cell and sealed.

***26°C Fixed Temperature Metatorbernite Phases.***

*higher relative humidity.*

This experiment demonstrated the effects that high relative humidity had on meta-torbernite at 26°C. Diffraction pattern MTB-1146 was taken when the relative humidity was 75.407% within the Kapton environmental cell (see Figure 12). Diffraction pattern MTB-1152 was taken approximately 83 minutes later when the relative humidity in the cell had dropped to 26.441%.

Diffraction patterns MTB-1146 and MTB-1152 revealed hydrated metatorbernite with intensity peaks for d-spacings 8.66 Å, 6.4 Å, and 5.4 Å. Further confirmation of the existence of metatorbernite hydrate was demonstrated by the absence in the diffraction patterns of its lesser hydrates with d-spacing 8.22 Å, 6.9 Å, and 5.3 Å intensity peaks.

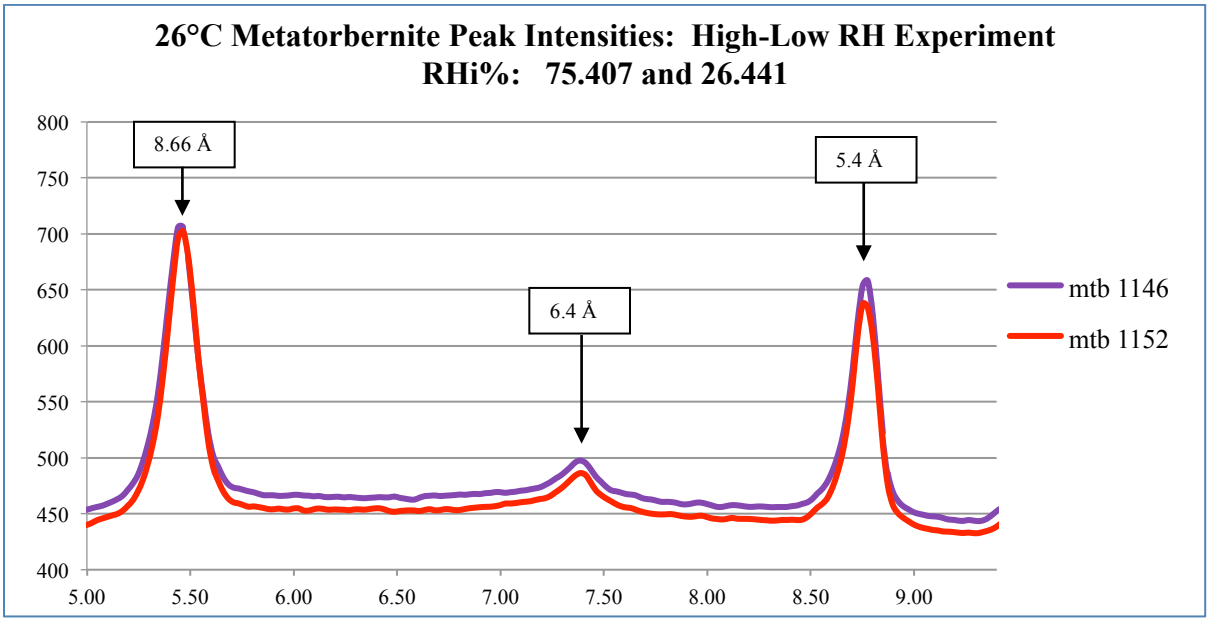


*Figure 12.* Metatorbernite without Lesser Hydrates.

The result of this experiment was consistent with the Bruker XRD Chamber 1 and Chamber 2 experiments. When the metatorbernite was switched from Chamber 1 to Chamber 2 (KCl 84.3% RH) to evaluate additional reconstitution of metatorbernite hydrate (see Figures 9 and 10), the difference between diffraction patterns MTB-1146 and MTB-1152 was statistically insignificant (see Figure 12), and this was due to the low activity of water ($a_{H_2O}$) in the reaction at room temperature (~24°C).

*low relative humidity.*

This experiment demonstrated the effect that low relative humidity had on metatorbernite at a fixed-point temperature of 26°C. When the relative humidity was further lowered from -1.746 to -1.811% from diffraction patterns MTB-1410 to MTB-1450, there was no change in the peak intensities for d-spacings 8.66 Å, 6.4 Å, and 5.4 Å (see Figure 13).

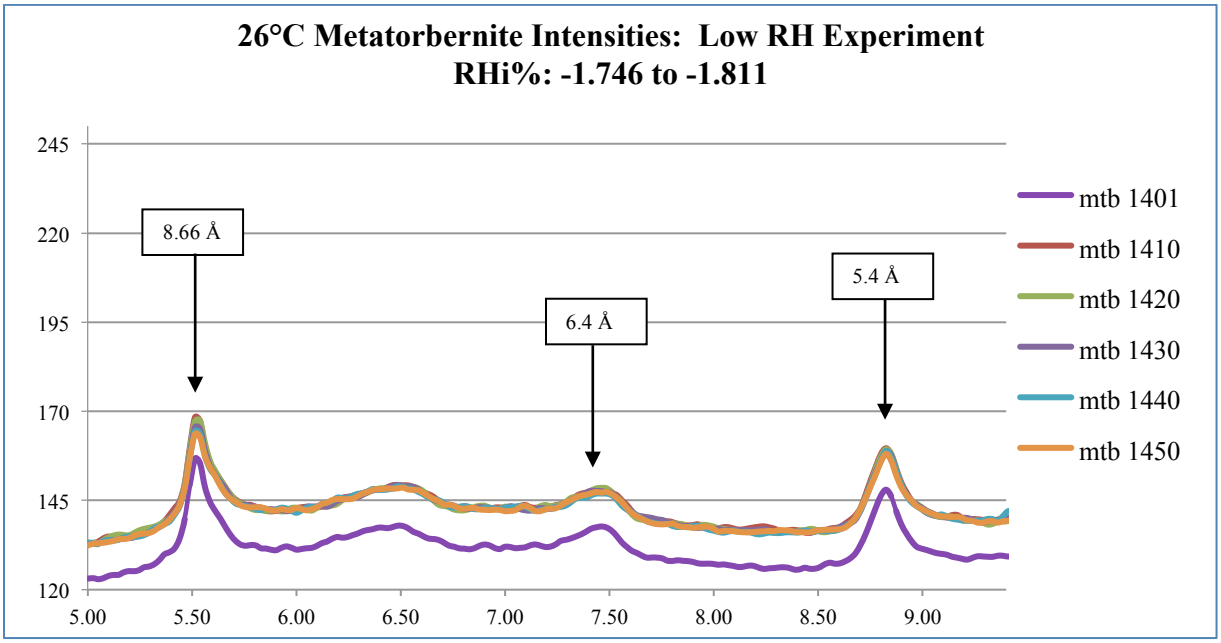


*Figure 13.* Metatorbernite without Lesser Hydrates.

As with the 26°C High RHi Experiment, the absence of lesser hydrates of metatorbernite with d-spacing 8.2 Å, 6.82 Å, and 5.3 Å peak intensities confirmed that only metatorbernite hydrate was present in the powder sample.

The result of this 26°C experiment was consistent with the Bruker XRD Chamber 2 (KCl 84.3% RH) experiment conducted at 24°C. When metatorbernite was switched from Chamber 2 to Chamber 1 (LiCl 11.3% RH) to evaluate for the formation of lesser hydrates of metatorbernite (see Figures 9 and 10) they were not present, and this was due to the low activity of water ($a_{H_2O}$) at RT 24°C.

### *36°C Fixed Temperature Metatorbernite Phases.*

*hydration of metatorbernite.*

The experiment began with a relative humidity of 37.876%. MTB-390 revealed intensity peaks with d-spacings 8.66 Å, 6.4 Å, and 5.4 Å that are consistent with metatorbernite hydrate

(see Figure 14). Further evidence of metatorbernite hydrate is the absence of d-spacings 8.3 Å, 6.9 Å, and 5.3 Å peak intensities that are indicative of lesser hydrates of metatorbernite.

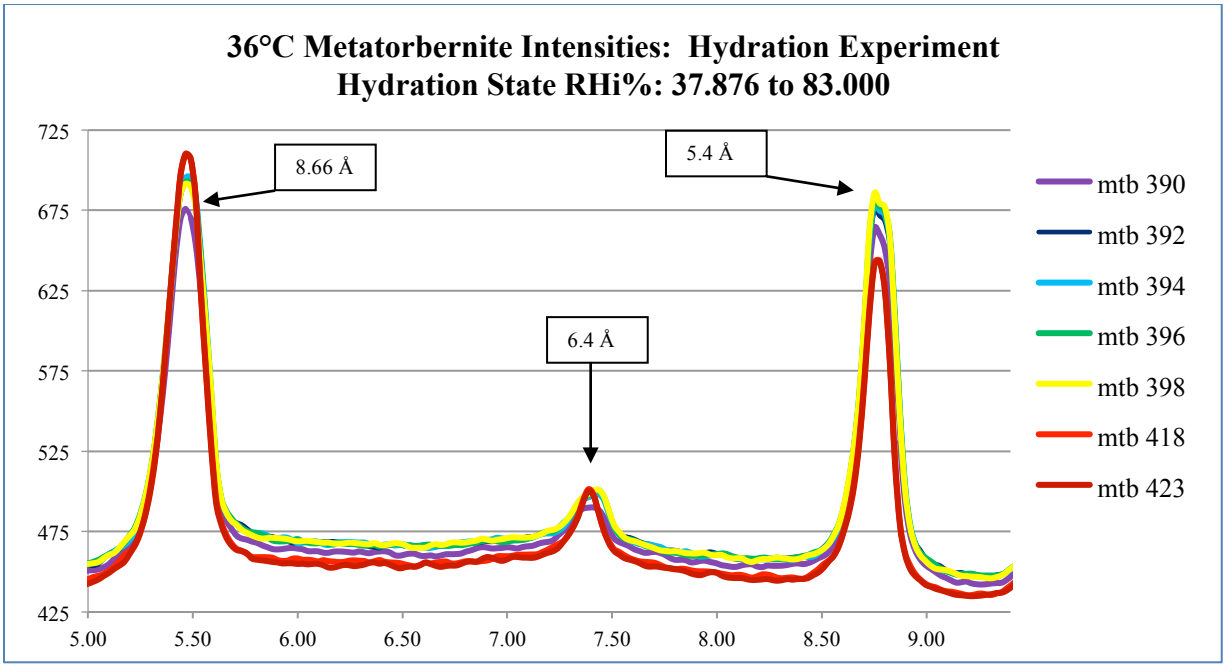


*Figure 14.* Hydration of Metatorbernite.

Incremental increases of relative humidity increased the intensity of d-spacing peaks 8.66 Å, 6.4 Å, and 5.4 Å from diffraction pattern MTB-392 through MTB-423 (see Figure 14). As the reaction continued, increased d-spacings 8.66 Å, 6.4 Å, and 5.4 Å peak intensities indicated that there was additional metatorbernite hydrate forming in the sample.

***64°C Fixed Temperature Metatorbernite Phases.***

The diffraction patterns in this experiment were taken through one dehydration cycle. Diffraction pattern MTB-344 with a relative humidity of -2.068% revealed two strong intensity peaks with basal spacings 8.66 Å and 5.4 Å. These peak intensities were accompanied by a very low intensity peak with basal spacing 6.4 Å.

Incremental reduction of relative humidity caused the 8.66 Å, 6.4 Å, and 5.4 Å peaks to lose intensity and develop shoulders on their right (smaller d-spacing) side (see Figure 15).

Development of shoulders indicated the onset of a transitional phase in the basal spacing of metatorbernite. As the relative humidity reduced, the 8.66 Å and 5.4 Å peak intensities in diffraction peaks MTB-345 through MTB-347 decreased. Once the relative humidity (RHi) dropped to less than -2.630%, the transitional phase ended and lesser hydrates of metatorbernite were evident in d-spacings 8.22 Å and 5.3 Å from diffraction pattern MTB-348 through MTB-350 (see Figure 15).

The results of this experiment demonstrated that structurally distinct phases occurred during transition conditions with a fixed-point temperature of 64°C and relative humidity values from -2.544 to -2.620. The diffraction patterns and their respective transitions for both basal spacings 8.66 Å to 8.2 Å and basal spacings 5.4 Å and 5.3 Å occurred at lower temperatures.

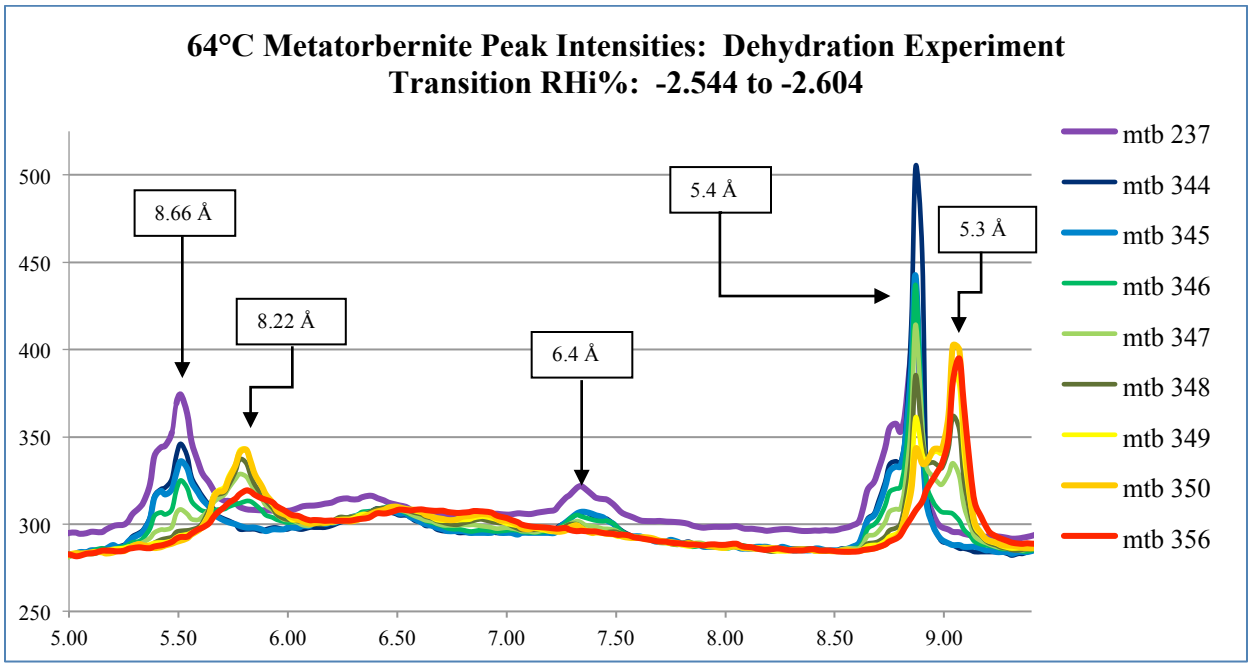


*Figure 15.* Metatorbernite Lesser Hydrates.

In this experiment, the transition and appearance of lesser hydrates of metatorbernite at lower temperatures were not in agreement with previous investigations by Stubbs et al. (2010)

and Suzuki et al. (2005). For example, the earlier research has shown that during transition conditions the lesser hydrates of metatorbernite occur at much higher temperatures.

***68°C Fixed Temperature Metatorbernite Phases.***

Diffraction patterns of metatorbernite were taken through one dehydration cycle that was followed by one rehydration cycle. The purpose of the rehydration cycle was to determine whether the dehydration state in the 64°C experiment was reversible. If metatorbernite was reversible by increasing relative humidity, lesser hydrate 8.22 Å, 6.9 Å, and 5.3 Å d-spacings would progressively disappear as metatorbernite reconstituted.

Diffraction pattern MTB-548 revealed intensity peaks with a d-spacings of 8.66 Å, 6.4 Å, and 5.4 Å that were consistent with metatorbernite (see Figure 16). The 8.66 Å and 5.4Å peaks began losing intensity from diffraction pattern MTB-568 through MTB-588 as the relative humidity was lowered, which was evidenced by the development of shoulders on their right (smaller d-spacing) side both between the 8.66 Å and 8.22 Å intensity peaks and between the 5.4 Å and 5.3 Å intensity peaks.

Lesser hydrates of metatorbernite with d-spacings 8.22 Å and 5.3 Å were visible from MTB-608 through MTB-628. The RHi measured from -1.186% to -2.125% during the transition conditions of the experiment (see Figure 16).

Metatorbernite was rehydrated by increasing the flow rate of wet helium gas. As rehydration progressed lesser hydrates of metatorbernite with d-spacings 8.22 Å and 5.3 Å intensity peaks transitioned and progressively disappeared. The continued formation of additional metatorbernite hydrate occurred at the expense of the lesser hydrate phases of metatorbernite. The reappearance of d-spacings 8.66 Å, 6.4 Å, and 5.4 Å from MTB-668 through MTB-698 indicated that metatorbernite hydrate was reconstituting.

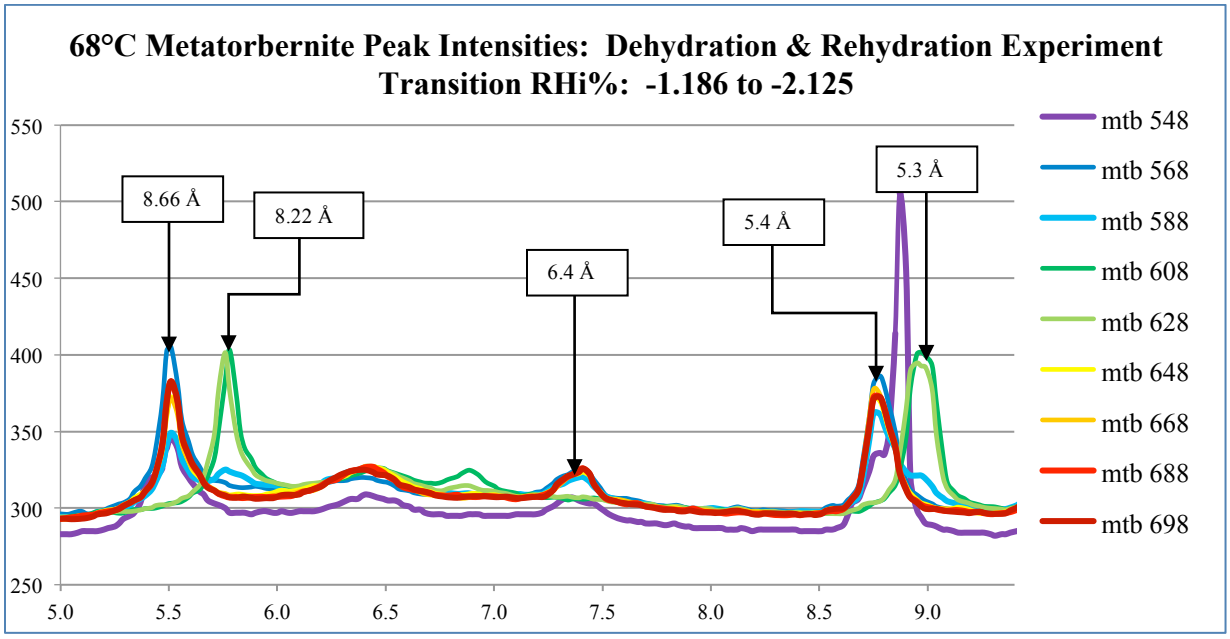


*Figure 16.* Metatorbernite with Lesser Hydrate D-spacings.

Rehydration of metatorbernite from its lesser hydrates, in this experiment, is a new finding that has not been demonstrated in previous research investigations. In addition, the temperatures at which lesser hydrates and their associated basal spacings appeared in this experiment were lower and not in agreement with previous investigations by Stubbs et al. (2010) and Suzuki et al. (2005).

***72°C Fixed Temperature Metatorbernite Phases.***

Diffraction patterns of metatorbernite were taken through one dehydration cycle that was followed by one rehydration-cooling cycle. Unlike the rehydration cycle in the 68°C experiment that only raised relative humidity (RHi), this experiment both raised the RHi and lowered the temperature to determine whether reconstitution of metatorbernite hydrate would take place.

Diffraction patterns were taken through one dehydration cycle that began with a relative humidity of 1.221%. Intensity peaks with d-spacings 8.66 Å, 6.4 Å, and 5.4 Å from diffraction

patterns MTB-720 through MTB-740 indicated metatorbernite hydrate was present (see Figure 17).

Incremental reduction of relative humidity caused the d-spacing 8.66 Å, 6.4Å, and 5.4 Å intensity peaks to lose intensity and develop shoulders on their right (smaller d-spacing) side. As with the 68°C experiment, the onset of a transitional phase with development of shoulders occurred both between the d-spacing 8.66 Å and 8.22 Å intensity peaks and between the d-spacing 5.4 Å and 5.3 Å intensity peaks.

Lesser hydrates of metatorbernite with d-spacings 8.22 Å and 5.3 Å persisted from MTB-760 through MTB-772 (see Figure 17). During the transition phase the 6.4 Å peak lost some intensity. The relative humidity (RHi) measured from -2.118% to -2.162%, during the transition conditions of the experiment.

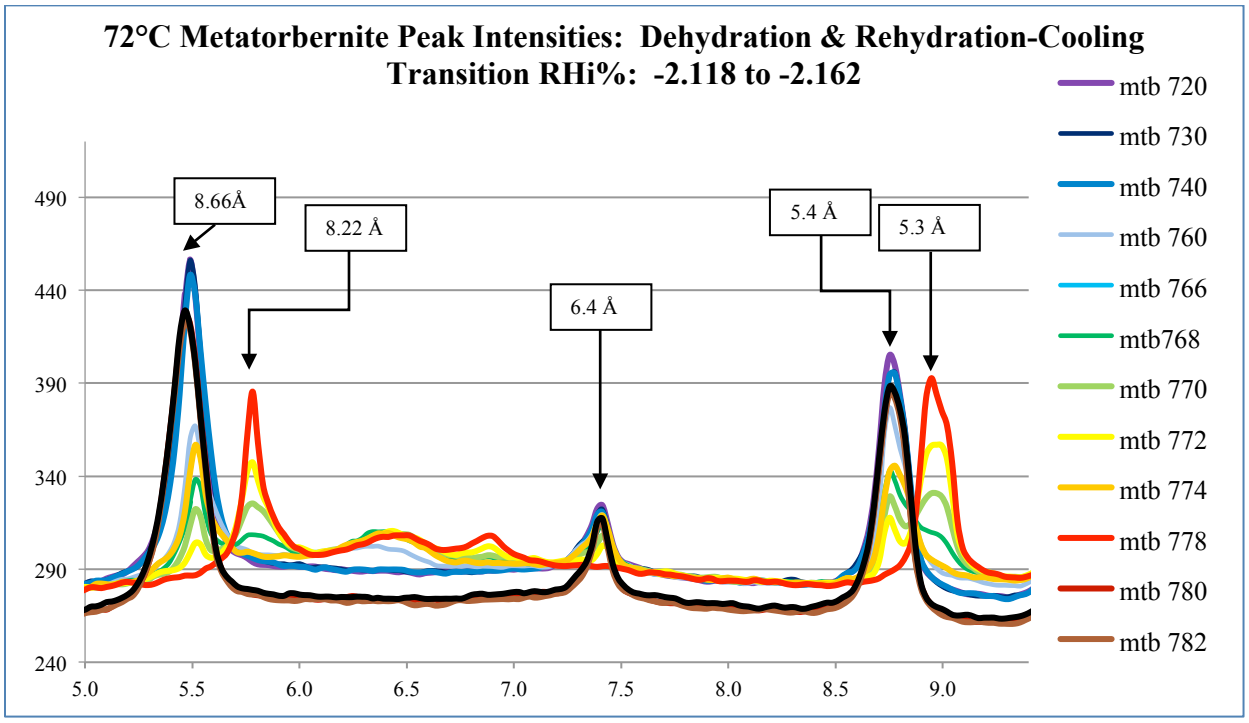


*Figure 17.* Metatorbernite and Lesser Hydrate D-spacings, Cooling and Rehydrating.

Reconstitution of metatorbernite hydrate began by cooling the sample to 35.061°C and increasing RHi to 39.670% for approximately one hour. As a result, the lesser hydrates of metatorbernite with d-spacing 8.22 Å and 5.3 Å intensity peaks progressively disappeared. This result indicated that reconstitution of metatorbernite hydrate had formed at the expense of lesser hydrates of metatorbernite. The 8.66 Å, 6.4 Å, and 5.4 Å d-spacing intensity peaks re-appeared when metatorbernite was cooled to 35°C and the RHi was increased to greater than 39.670%.

The results of the experiment demonstrate that structurally distinct transition phases producing lesser hydrates of metatorbernite occur with incremental reduction in relative humidity values.

***76°C Fixed Temperature Metatorbernite Phases.***

The diffraction patterns were taken through one dehydration cycle. MTB-808 revealed d-spacing 8.66 Å, 6.4 Å, and 5.4 Å intensity peaks that were consistent with metatorbernite hydrate. Incremental reduction of the relative humidity caused d-spacing 8.66 Å, 6.4 Å, and 5.4 Å peaks to lose intensity and develop shoulders on their right (smaller d-spacing) side from patterns MTB-813 through MTB-841 (see Figure 18).

The onset of a transitional phase occurred both between d-spacings 8.66 Å and 8.22 Å intensity peaks and between d-spacings 5.4 Å and 5.3 Å that persisted from patterns MTB-845 through MTB-880. During this transition phase the 6.4 Å peak continued to lose intensity. In diffraction pattern MTB-890, the 8.22 Å and 6.4 Å intensity peaks progressively disappeared to complete extinction leaving only a progressively disappearing 5.3 Å intensity peak. The RHi measured from -1.952% to -2.083%, during the transition conditions of the experiment.

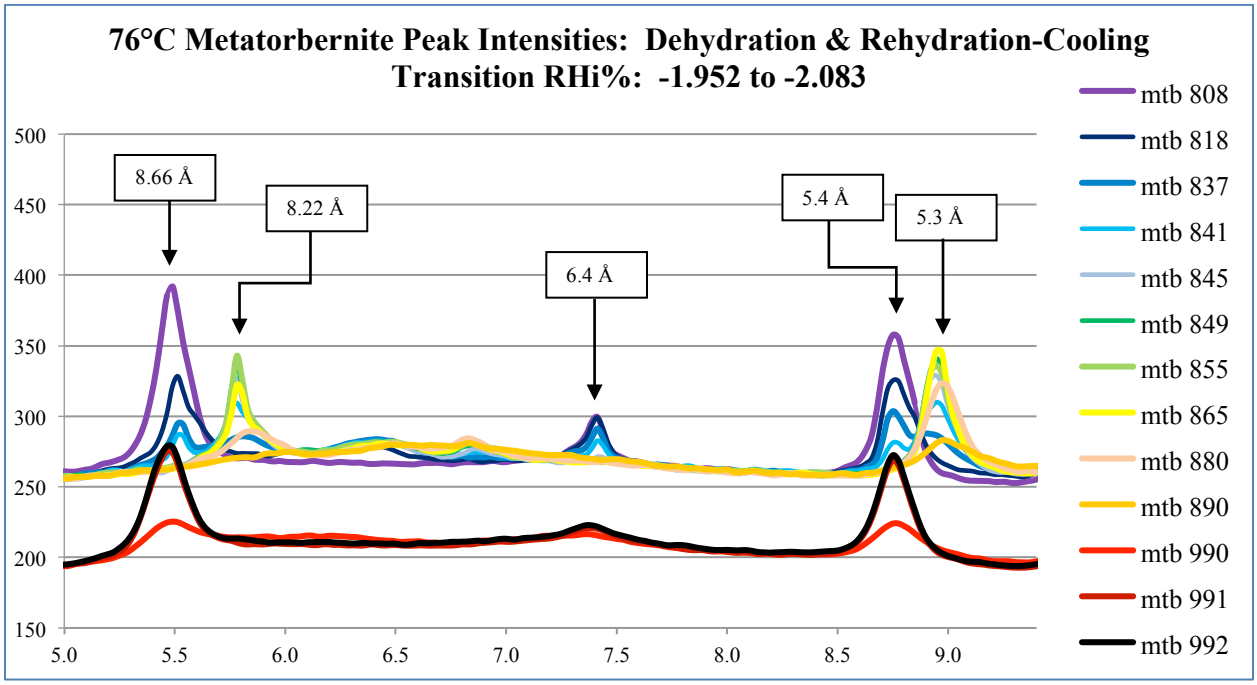


*Figure 18.* Metatorbernite and Lesser Hydrate D-spacings, Cooling and Rehydrating.

Reconstitution of metatorbernite hydrate began by cooling and re-hydrating the sample to 46.412°C and RHi 25.335% for approximately five minutes. Diffraction patterns MTB-990 through MTB-992 indicated that lesser hydrates of metatorbernite with d-spacing 8.22 Å and 5.3 Å intensity peaks transitioned and progressively disappeared (see Figure 18). Consistent with results of the 68°C and72°C experiments, this experiment demonstrated that reconstitution of metatorbernite hydrate with d-spacing 8.66 Å, 6.4Å, and 5.4 Å intensity peaks had formed at the expense of lesser hydrates of metatorbernite.

### *80°C Fixed Temperature Metatorbernite Phases.*

*dehydration.*

Diffraction patterns were taken through one dehydration cycle that began 1.014% relative humidity. MTB-1021 revealed intensity peaks with basal spacings 8.66 Å, 6.4 Å, and 5.4 Å (see Figure 19). Incremental reduction of the relative humidity caused the 8.66 Å and 5.4 Å peaks to

begin to lose intensity and develop shoulders on their right (smaller d-spacing) side from pattern MTB-1050 through MTB-1056.

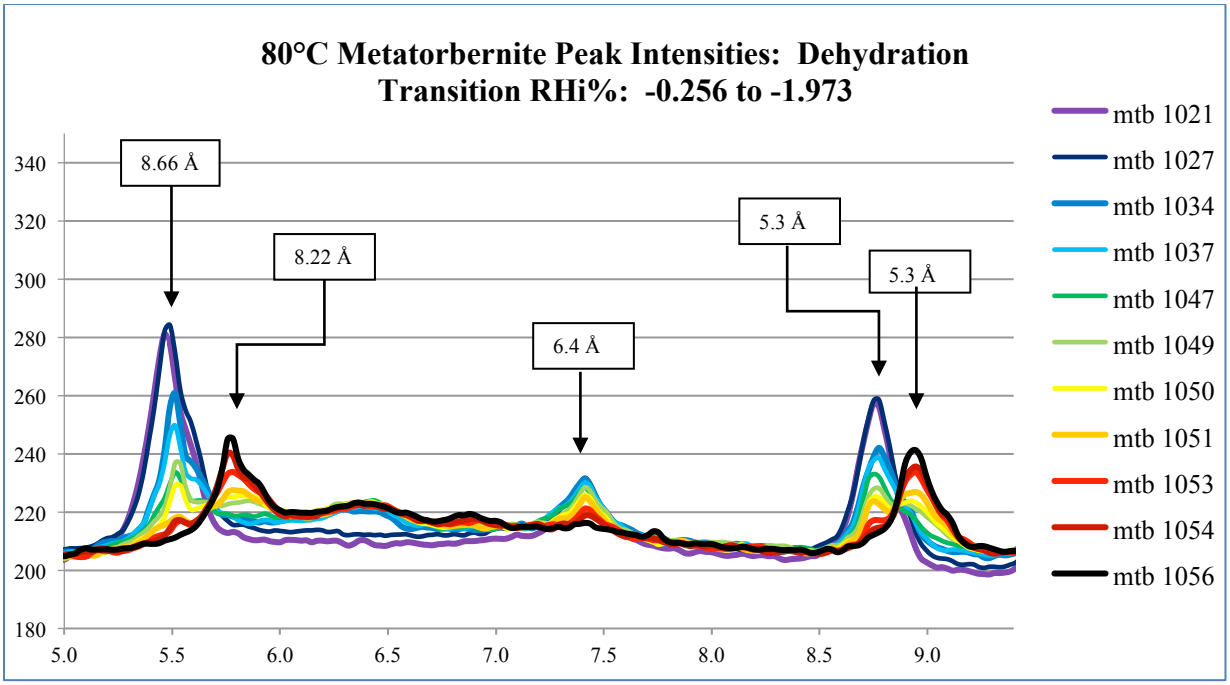


*Figure 19.* Metatorbernite and Lesser Hydrate D-spacing, Dehydrating.

A transitional phase with development of shoulders occurred both between d-spacings 8.66 Å and 8.22 Å peaks and between d-spacings 5.4 Å and 5.3 Å peaks that persisted from MTB-1027 through MTB-1056 (see Figure 19). The fixed-point temperature was 80°C with RHi from -0.256% to -1.973%, during the transition conditions.

The results of the experiment demonstrated that structurally distinct transition phases occurred with incremental reduction in relative humidity values. Any further reduction in the relative humidity beyond the transition phase in MTB-1056 resulted in the extinction of d-spacing 8.66 Å, 8.22 Å and 6.4 Å intensity peaks. This may be due to the increase in temperature coupled with reduction of relative humidity below -1.973%, which may cause the destruction of the sample, due to fracturing of the metatorbernite crystals and overall damage to the unit cell structure.

*rehydration-cooling.*

Reconstitution of metatorbernite hydrate began by cooling and re-hydrating the sample to 27.029°C and RHi 75.098% respectively for approximately nine minutes. Subsequent diffraction patterns MTB-1132 through MTB-1144 indicated that lesser hydrates of metatorbernite with d-spacing 8.22 Å, 6.9 Å, and 5.3 Å intensity peaks progressively disappeared (see Figure 20 compared with Figure 19).

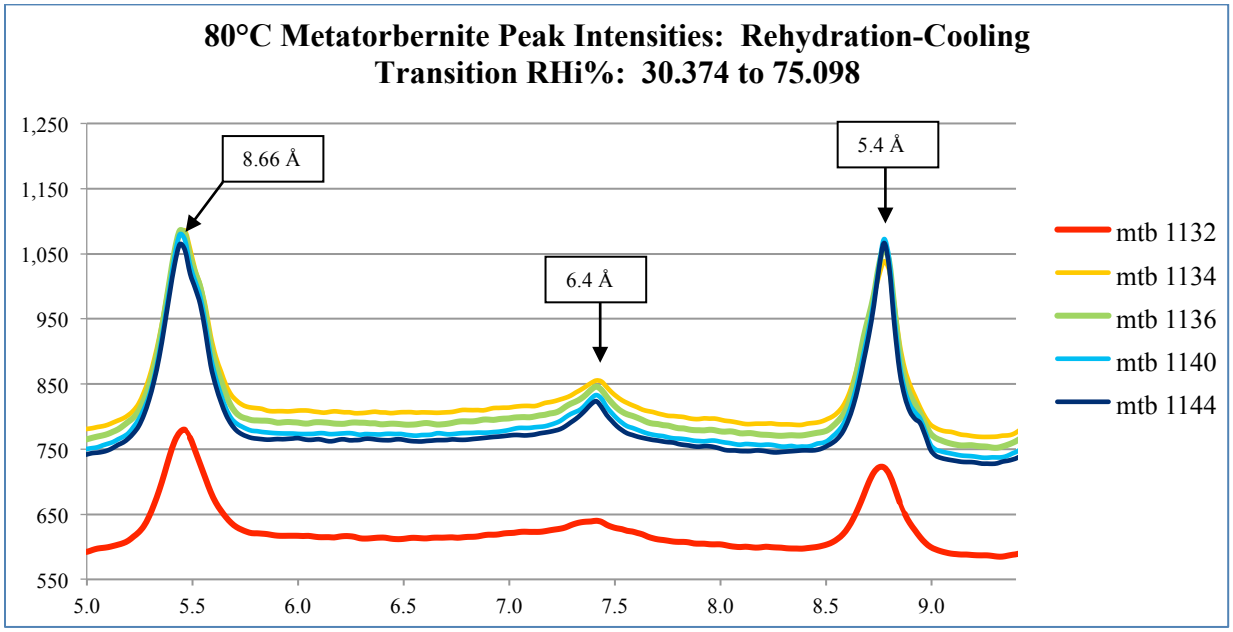


*Figure 20.* 80°C Metatorbernite Cooling and Rehydrating.

Consistent with results of previous dehydration and rehydration-cooling experiments, reconstitution of metatorbernite hydrate with d-spacing 8.66 Å, 6.4Å, and 5.4 Å intensity peaks formed at the expense of lesser hydrates of metatorbernite.

***84°C Fixed Temperature Metatorbernite Phases.***

Diffraction patterns were taken through one dehydration cycle that began with 0.321% RHi. MTB-1170 revealed intensity peaks with d-spacings 8.66 Å, 6.4 Å, and 5.4 Å and were consistent with metatorbernite hydrate. During MTB-1208 through MTB-1216, an intensity

peak with d-spacing 6.9 Å appeared. The appearance of this peak was consistent with the results of the Bruker XRD heating experiments. Incremental reduction of the relative humidity caused the 8.66 Å and the 5.4 Å peaks to begin losing intensity. A transitional phase with development of shoulders on their right (smaller d-spacing) side occurs between both the 8.66 Å and 8.22 Å peaks and the 5.4 Å and 5.3 Å peaks that persisted from MTB-1170 through MTB-1188 (see Figure 21). The RHi during the transition measured from -1.348% to -1.888%.

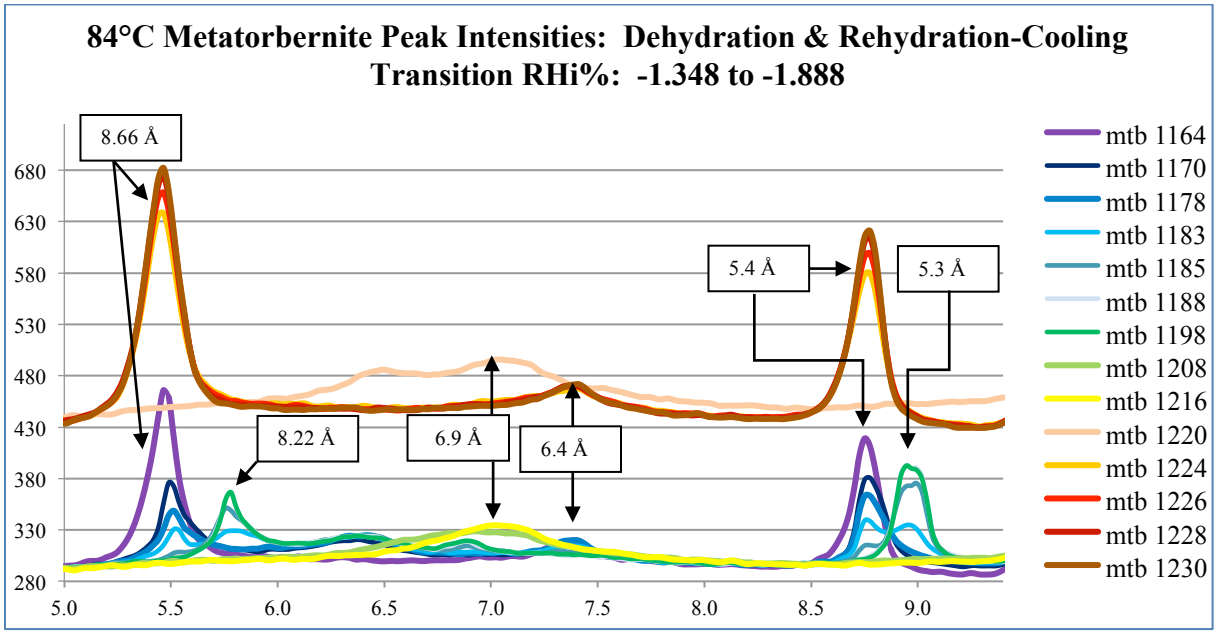


*Figure 21.* 84°C Metatorbernite Dehydration, Followed By Cooling and Rehydrating.

The results of the dehydration phase of the experiment were similar to the 80°C experiment in that structurally distinct lesser hydrates of metatorbernite occurred with incremental reduction in relative humidity. Further reduction in relative humidity, beyond diffraction pattern MTB-1198, resulted in the disappearance of d-spacings 8.6 Å, 6.4 Å, and 5.4 Å intensity peaks.

Reconstitution of metatorbernite hydrate began by cooling the sample and re-hydrating it to 34.427°C and RHi 42.251% for approximately nineteen minutes. Subsequent diffraction

patterns from MTB-1224 through MTB-1230 indicated that lesser hydrates of metatorbernite with d-spacing 8.22 Å, 6.9 Å, and 5.3 Å intensity peaks had progressively disappeared (see Figure 21). Diffraction pattern MTB-1224 indicated that metatorbernite hydrate had reconstituted.

Consistent with the results of previous dehydration and rehydration-cooling experiments in this investigation, reconstitution of metatorbernite hydrate with d-spacing 8.66 Å, 6.4Å, and 5.4 Å intensity peaks formed at the expense of lesser hydrates of metatorbernite.

***100°C Fixed Temperature Metatorbernite Phases.***

The diffraction patterns were taken through one dehydration cycle from MTB-1303 through MTB-1400. MTB-1303 revealed an intensity peak with d-spacing 6.9 Å that indicated a lesser hydrate of metatorbernite (see Figure 22). The peak intensities of lesser hydrates of metatorbernite with d-spacings 8.22 Å and 5.3 Å were not visible in diffraction patterns MTB-1303 through MTB-1400.

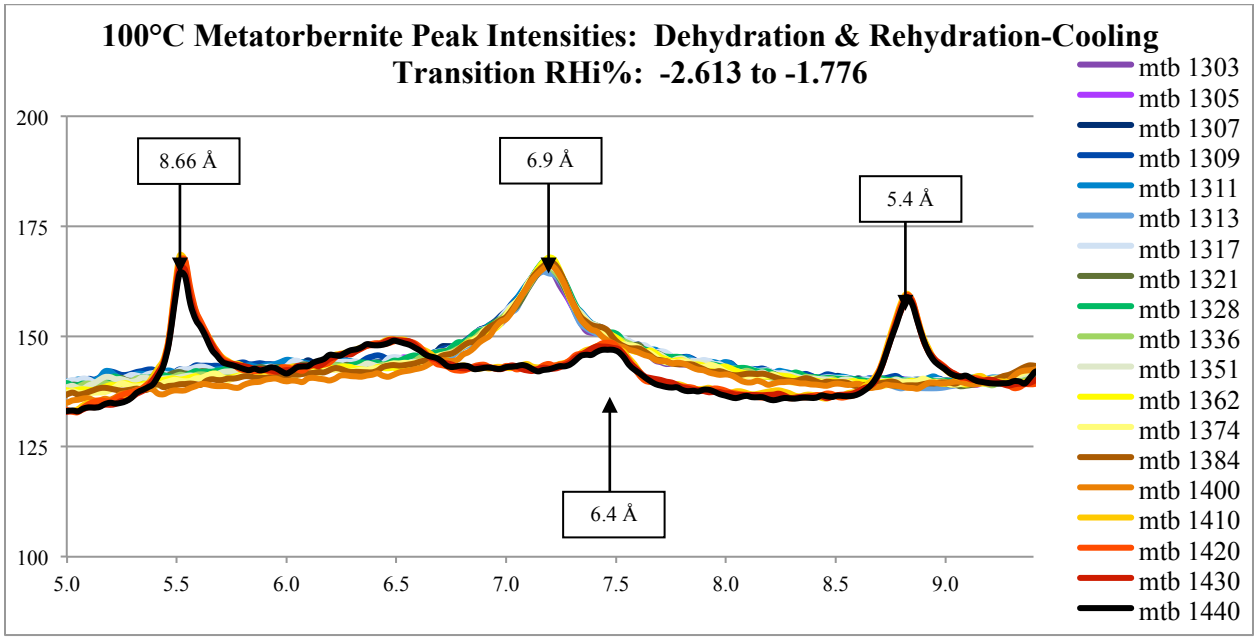


*Figure 22.* 100°C Metatorbernite Cooling, While Rehydrating.

The dehydration cycle was followed by a combined rehydration-cooling cycle. Diffraction patterns MTB-1400 through MTB-1410 were collected over the next 37 minutes, while the temperature lowered from 42°C to 26°C and RHi raised from -2.613% to -1.776%. During this time d-spacing 6.9 Å progressively disappeared, without the appearance of other lesser hydrates with d-spacings 8.22 Å and 5.3 Å.

The rehydration-cooling experiment from diffraction patterns MTB-1420 through MTB-1440, demonstrated reconstitution of metatorbernite hydrate with d-spacing 8.66 Å, 6.4 Å, and 5.4 Å intensity peaks. These metatorbernite hydrate intensity peaks formed at the expense of the 6.9 Å d-spacing lesser hydrate, which was the lesser hydrate present in the diffraction pattern at 100°C. These results were consistent with Bruker XRD Heating Experiments 2 (150°C) and 3 (140°C).

**Discussion**

This is the first work to investigate the role of water activity ($a_{H_2O}$) or probe the reversibility of metatorbernite dehydration. The results of these experiments have elucidated a variety of possible d-spacings and peak intensities that metatorbernite and its lesser hydrates can exhibit under specific temperature and relative humidity conditions. In addition, the results of this investigation were both consistent and repeatable.

A particularly important result found in both the Bruker and Advanced Photon Source (APS) experiments indicated that lesser hydrates of metatorbernite with d-spacings 8.3 Å, 6.9 Å, and 5.3 Å appeared at lower temperatures than previously demonstrated in Stubbs et al. (2010), Suzuki et al. (2005), and Locock & Burns, (2003). A second critical result and new finding demonstrated is that the dehydration reactions are reversible.

The results of these experiments determined that when metatorbernite hydrate was heated to greater than or equal to 64°C, lesser hydrates of metatorbernite with d-spacings 8.3 Å, 6.9 Å, and 5.3 Å peak intensities progressively appeared. When metatorbernite was further heated to greater than or equal to 84°C the d-spacing 6.9 Å peak continued to increase in intensity, while d-spacings 8.3 Å and 5.3 Å peaks progressively disappeared.

During this investigation, metatorbernite was incrementally cooled to determine if phase changes were occurring. During the cooling process, metatorbernite's lesser hydrates with d-spacings 8.3 Å, 6.9 Å, and 5.3 Å reconstituted back to metatorbernite hydrate with d-spacings 8.6 Å, 6.4 Å, and 5.4 Å. The reversal of the transition conditions back to room temperature indicated that lesser hydrates of metatorbernite were reconstituting to its hydrated state at the expense of the lesser hydrates. The finding of reversibility was consistent with rehydration-cooling experiments performed by both the Bruker XRD and the APS.

**Implications**

Understanding of uranium migration in the subsurface and remediation of already contaminated sites is a fundamental step in planning related to nuclear facilities. The growing recognition of the importance of uranyl phosphates in the subsurface uranium budget in oxidizing regions places a premium on identifying and understanding the occurrence of these complex phases. Recent planning for remediation of contaminated sites at the DOE's Hanford facility includes subsurface phosphate amendments aimed at inducing meta-autunite group mineral precipitation as an important strategy for the immobilization of actinides (Vermeul et al., 2008, 2009; Wellman et al., 2008, 2010). A critical step in such planning is incorporation of realistic phase relations for the solid phases. Despite the recognition of multiple, complex

dehydration transformations in autunite/meta-autunite group minerals for over a hundred years, a significant knowledge gap remains concerning the occurrence of these phases.

This study focused on what are likely the most important parameters controlling autunite/meta-autunite group dehydration reactions: temperature and activity of water ($a_{H_2O}$). Leveraging the prior work of Stubbs et al. (2010) and focusing on the occurrences at Hanford, this study centered on the phase relations of the Cu meta-autunite mineral, metatorbernite and its lesser hydrates.

**References**

Arai, Y., Marcus, M.K., Tamura, N., Davis, J.A., and Zachara, J.M. (2007). Spectroscopic evidence for uranium bearing precipitates in vadose zone sediments at the Hanford 300-area site. *Environmental Science and Technology*, *41*, 4633-4639.

Buck, E.C., Dietz, N.L., and Bates, J.K. (1995). Uranium-contaminated soils—ultramicrotomy and electron-beam analysis. *Microscopy Research and Technique, 31,* 174–181.

Buck, E.C., Brown, N.R., and Dietz, N.L. (1996). Contaminant uranium phases and leaching at the Fernald site in Ohio. *Environmental Science and Technology, 30*, 81–88.

Catalano, J.G., McKinley, J.P., Zachara, J.M., Heald, S.M., Smith, S.C., and Brown G.E. (2006). Changes in uranium speciation through a depth sequence of contaminated Hanford sediments. *Environmental Science and Technology*, *40*, 2517-2524.

Crowley, K.D. (2007). *Science and Technology needs for DOE Site Cleanup: Workshop Summary.* National Academy Press, Washington, DC. Department Of Energy (1997). *Linking Legacies: Connecting the Cold War Nuclear Weapons Production Process to Their Environmental Consequences,* DOE/EM-0319, USDOE.

Finch, R.J. and Murakami, T. (1999). Systematics and paragenesis of uranium minerals. *In* Uranium: Mineralogy, Geochemistry and the Environment (P.C. Burns and R.J. Finch, Eds.). Mineralogical Society of America and Geochemical Society, *Reviews in Mineralogy and Geochemistry*, *38*, 91-179.

Greenspan, L. (1977). Humidity fixed points of binary saturated aqueous solutions. *Journal of Research of the National Bureau of Standards*, *81A*(1), 91-93.

Hammersley, A.P., Svensson, S.O., Hanfland, M., Fitch, A.N., & Hausermann, D. (1996). Two-dimensional detector software: From real detector to idealised image or two-theta scan. *High Pressure Research*, *14*, 235-248.

Jerden, J.L., & Sinha, A.K. (2003). Phosphate based immobilization of uranium in an oxidizing bedrock aquifer. *Applied Geochemistry*, *18*, 823–843.

Jerden, J.L., Sinha, A.K., & Zelazny, L. (2003). Natural immobilization of uranium by phosphate mineralization in an oxidizing saprolite-soil profile: chemical weathering of the Coles Hill uranium deposit, Virginia. *Chemical Geology, 199*, 129–157.

Locock, A. J., & Burns, P.C. (2003). Crystal structures and synthesis of the copper-dominant members of the autunite and meta-autunite groups: Torbernite, zeurenerite, metatorbernite and metazeunerite. *Canadian Mineralogist, 41,* 489-502.

Murakami, Takashi. (2006). *Actinides 2005-Basic Science, Applications and Technology.* Materials Research Society Symposium Proceedings, *893*, 273-281.

Murakami, T., Ohnuki, T., Isobe, H., & Sato, T. (1997). Mobility of uranium during weathering. *American Mineralogist, 82,* 888-899.

Murakami, T., Sato, T., Ohnuki, T., & Isobe, H. (2005). Field evidence for uranium nanocrystallization and its implications for uranium transport. *Chemical Geology, 221,* 117-126.

National Research Council (U.S.). Crowley, K. D., and National Research Council (U.S.). (2010). *Science and technology for DOE site cleanup: Workshop summary*. Washington, D.C: National Academies Press.

Nuclear Regulatory Commission (U.S.). (March 2011). *High level waste.* Retrieved on July 6, 2011 from http://www.nrc.gov/waste/high-level-waste.html

Rinne, F. (1901). Kalkuranit uncl seine Entwdsserungsprodukte (Metakalkuranite)t Centralblatt Fur Mineralogie, 709.

Ross, M., Evans, H.T., & Appleman, D.E. (1964). Studies of torbernite minerals 2. Crystal structures of meta-torbernite. *American Mineralogist, 49,* 1603-1621.

Sato, T., Murakami, T., Yanase, N., Isobe, H., Payne, T.E., & Airey, P.L. (1997) Iron nodules scavenging uranium from groundwater. *Environmental Science and Technology*, *31*, 2854–2858.

Singer, D.M., Zachara, J.M., & Brown, G.E. (2009). Uranium speciation as a function of depth in contaminated Hanford Sediments: A micro-XRF, micro-XRD, and micro- and bulk-XAFS study. *Environmental Science and Technology*, *43*, 630-636.

Stergiou, A.C., Rentzeperis, P.J., & Sklavounos, S. (1993). Refinement of the crystal-structure of metatorbernite. *Zeitschrift für Kristallographie, 205,* 1-7.

Stubbs, J.E. (2009) Mineralogical and geochemical studies of uranium-contaminated soils and uranium phosphate minerals. Ph.D. thesis, Johns Hopkins University, Baltimore, Maryland.

Stubbs, J.E., Elbert, D.C., Veblen, D.R., & Zhu, C. (2006). Electron microbeam investigation of uranium-contaminated soils from Oak Ridge, Tennessee, U.S.A. *Environmental Science and Technology, 40,* 2108–2113.

Stubbs, J.E., Elbert, D.C., Veblen, L.A., & Veblen, D.R. (2007). Rapid cation depletion during electron microprobe analysis of uranium phosphates. Eos Transactions AGU, 88, Fall Meeting Supplemental, Abstract V51A-0324.

Stubbs, J.E., Veblen, L.A., Elbert, D.C., Zachara, J.M., Davis, J.A., & Veblen, D.R. (2009). Newly recognized hosts for uranium in the Hanford Site vadose zone. Geochimica et Cosmochimica Acta, 73, 1563–1576.

Stubbs, J. E., Post, J. E., Elbert, D. C., H., Peter J., & Veblen, D. R. (2010). Uranyl phosphate sheet reconstruction during dehydration of metatorbernite [Cu(UO2)2(PO4)2 • 8H2O]. *American Minerologist*, 95, 1132-1140.

Suzuki, Y., Murakami, T., Kogure, T., Isobe, H., & Sato, T. (1998). Crystal chemistry and microstructures of uranyl phosphates. Materials Research Society Symposia Proceedings, 506, 839–846.

Suzuki, Y., Sato, T., Isobe, H., Kogure, T., & Murakami, T. (2005). Dehydration processes in the meta-autunite group minerals meta-autunite, metasaleeite, and metatorbernite. *American Mineralogist*, 90, 1308–1314.

Takano, Y. (1961). X-ray study of autunite. *American Mineralogist, 46,* 812–822.

Vermeul, V.R., Fruchter, J.S., Fritz, B.G., Mackley, R.D., Wellman, D.M., & Williams, M.D. 2008. In-Situ Uranium Stabilization through Polyphosphate Injection: Pilot-Scale Treatability Test at the 300 Area, Hanford Site. Pacific Northwest National Laboratory, PNNL-SA-58147, Richland, Washington.

Vermeul, V.R., Bjornstad, B.N., Fritz, B.G., Fruchter, J.S., Mackley, R.D., Newcomer, D.R., Mendoza, D.P., Rockhold, M.L., Wellman, D.M., & William, M.D. (2009). 300 Area Uranium Stabilization Through Polyphosphate Injection: Final Report. Pacific Northwest National Laboratory, PNNL-18529, Richland, Washington.

Walker, G. W. & Osterwald, F. W., (1956). Classification and distribution of uranium-bearing veins in the United States. United States Geological Survey. Wellman, D. M., Gunderson, K.M., Icenhower, J.P., & Forrester, S.W. (2007). Dissolution kinetics of synthetic and natural meta-autunite minerals, $X_3$-n(n)+ [$(UO_2)(PO_4)$]2 $xH_2O$, under acidic conditions. *Geochemistry Geophysics Geosystems, 8*, Q11001.

Wellman, D.M., Pierce, E.M., Richards, E.L., Fruchter, J.S., & Vermeul, V.R. (2008). Uranium Plume Treatability Demonstration at the Hanford Site 300 Area: Development of Polyphosphate Remediation Technology for In-Situ Stabilization of Uranium - 8070. In Waste Management 2008: HLW, TRU, LLW/ILW, *Mixed, Hazardous Wastes & Environmental Management,* 1-15. Arizona Board of Regents, Tucson, Arizona.

Wellman, D. M., McNamara, B. K., Bacon, D. H., Cordova, E. A., Ermi, R. M., Top, & L. M. (2009). Dissolution kinetics of metatorbernite under circum-neutral to alkaline conditions. *Environmental Chem*istry, *6*, 551– 560.

Wellman D,M., Fruchter, J.S., Vermeul, V.R., Richards, E.L., Jansik, D.P., & Edge, E. (2011). Evaluation of the efficacy of polyphosphate remediation technology: Direct and indirect remediation of uranium under alkaline conditions. *Technology and Innovation 13*(2):151-164. doi:10.3727/194982411X13085939956544

Zachara J.M., Serne, J., Freshley, M., Mann, F., Anderson, F., Wood, M., Jones, T., & Meyers, D. (2007). Geochemical processes controlling migration of tank wastes in Hanford's vadose zone. Vadose Zone Journal, *6*, 985-1003.

Zachara J.M., Davis, J.A., Liu, C., McKinley, J.P., Qafoku, N., Wellman, D.M., & Yabusaki, S.B. (2005). Uranium Geochemistry in Vadose Zone and Aquifer Sediments from the 300 Area Uranium Plume. Northwest National Laboratory, PNNL-15121, Richland, Washington.